Article

Discovery and Biophysical Characterization of 2-Amino-Oxadiazoles as Novel Antagonists of PqsR, an Important Regulator of Pseudomonas aeruginosa Virulence

Michael Zender, Tobias Klein, Claudia Henn, Benjamin Kirsch, Christine K. Maurer, Dagmar Kail, Christiane Ritter, Olan Dolezal, Anke Steinbach, and Rolf W. Hartmann

J. Med. Chem., **Just Accepted Manuscript** • DOI: 10.1021/jm400830r • Publication Date (Web): 06 Aug 2013

Discovery and Biophysical Characterization of 2-Amino-Oxadiazoles as Novel Antagonists of PqsR, an Important Regulator of *Pseudomonas aeruginosa* Virulence

AUTHOR NAMES

Michael Zender,[1] Tobias Klein,[1,†] Claudia Henn,[1,‡] Benjamin Kirsch,[1] Christine K. Maurer,[1] Dagmar Kail,[2] Christiane Ritter,[3] Olan Dolezal,[4] Anke Steinbach,[1] Rolf W. Hartmann[1,5]*

AUTHOR ADDRESS

[1]Helmholtz-Institute for Pharmaceutical Research Saarland, Department of Drug Design and Optimization, Campus C2.3, 66123 Saarbrücken, Germany

[2]PharmBioTec GmbH, Campus C2.2, 66123 Saarbrücken, Germany

[3]Helmholtz Centre for Infection Research, Department of Macromolecular Interactions, Inhoffenstraße 7, 38124 Braunschweig, Germany

[4]Commonwealth Scientific and Industrial Research Organization (CSIRO), Materials Science and Engineering, 343 Royal Parade, Parkville 3052 Victoria, Australia

[5]Pharmaceutical and Medicinal Chemistry, Saarland University, Campus C2.3, 66123 Saarbrücken, Germany

ABSTRACT

The human pathogen *Pseudomonas aeruginosa* employs alkyl quinolones for cell-to-cell communication. The *Pseudomonas* Quinolone Signal (PQS) regulates various virulence factors *via* interaction with the transcriptional regulator PqsR. Therefore, we consider the development of PqsR antagonists a novel strategy to limit the pathogenicity of *P. aeruginosa*. A fragment identification approach using surface plasmon resonance screening led to the discovery of chemically diverse PqsR ligands. The optimization of the most promising hit (**5**) resulted in the oxadiazole-2-amine **37** showing pure antagonistic activity in *E. coli* (EC_{50} 7.5 μM) and *P. aeruginosa* (38.5 μM) reporter gene assays. **37** was able to diminish the production of the PQS precursor HHQ in a PqsH deficient *P. aeruginosa* mutant. The level of the major virulence factor pyocyanin was significantly reduced in wild-type *P. aeruginosa*. In addition, site-directed mutagenesis in combination with isothermal titration calorimetry and NMR INPHARMA experiments revealed that the identified ligands bind to the same site of PqsR by adopting different binding modes. These findings will be utilized in a future fragment growing approach aiming at novel therapeutic options for the treatment of *P. aeruginosa* infections.

INTRODUCTION

Our view of bacterial lifestyle has changed drastically in the last few years. In the past, bacteria were deemed to be autonomous unicellular organisms. Nowadays, it is increasingly recognized that they have the ability to communicate with each other. A particular form of bacterial communication is referred to as *quorum sensing* (QS). QS functions *via* the release of signaling molecules. The concentration of these molecules increases as a function of cell density. After a threshold concentration has been reached they regulate gene expression in bacteria by activation of corresponding transcriptional regulators. QS cell-to-cell communication enables bacteria to monitor population density and to orchestrate their behavior on a population-wide scale.[1,2]

Pseudomonas aeruginosa, a Gram-negative opportunistic pathogenic bacterium is an important causative agent of nosocomial infections[3,4] and is involved in several acute and chronic infections. It is one of the major pathogens causing pneumonia e.g. in people suffering from cystic fibrosis.[5] The ability of *P. aeruginosa* to form biofilms contributes to its low antibiotic susceptibility mainly due to lowered metabolic activity and decreased growth rate of biofilm bacteria.[6] Moreover, during the last decades, *P. aeruginosa* strains resistant against nearly all established antibiotics have emerged, necessitating alternative therapeutic options.[7,8]

P. aeruginosa coordinates group behaviours *via* three interconnected QS circuitries. The *las*[9,10]and *rhl*[11,12] communication systems operate *via N*-acylated homoserine lactones (AHLs), which are prevalent signaling molecules in Gram-negative bacteria. In contrast, the *pqs* system[13,14] is restricted to particular *Pseudomona*s and *Burkholderia* strains.[15] It functions *via* the 2-alkyl-4(1*H*)-quinolones (HAQ) signal molecules PQS (*Pseudomonas* Quinolone Signal; 2-

heptyl-3-hydroxy-4(1*H*)-quinolone) and its precursor HHQ (2-heptyl-4(1*H*)-quinolone; Figure 1).

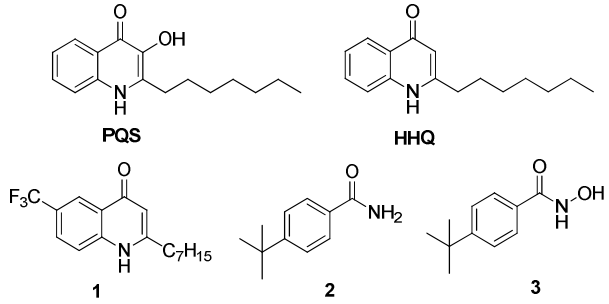

Figure 1: Structure of the *P. aeruginosa* signaling molecules PQS and HHQ as well as recently published PqsR ligands

Both interact with their receptor PqsR[16,17] to control many genes involved in the production of various virulence factors like elastase, pyocyanin and lectins.[18] Moreover, PQS enhances its own biosynthetic pathway by positively regulating the *pqsABCD(E)*[16,19,20] and *phnAB*[14] operons as well as it influences biofilm formation.[18,21] The discovery of QS systems in pathogenic bacteria provides novel options for inhibiting the virulence without interfering with bacterial viability.[22] The interference with QS systems by synthetic inhibitors[23] and the reduction of virulence factors by flucytosine[24] resulted in diminished *P. aeruginosa* pathogenicity in mouse pulmonary infection models demonstrating the in-vivo relevance of these anti-virulence strategies. Regarding *P. aeruginosa*, we consider PqsR - a key player for its pathogenicity - an attractive drug target. PqsR, also known as multiple virulence factor regulator (MvfR), belongs to the family of LysR-type transcriptional regulators (LTTR).[17] The N-terminal region contains a helix-turn-helix DNA binding motif and the C-terminus between amino acids 92-298 encodes for a predicted ligand binding domain (LBD).[17]

Recently, we have reported on the discovery of two different classes of antagonists which target PqsR (Figure 1). The HHQ derivative **1**[25] is a potent PqsR antagonist, but shows insufficient drug-like properties such as low aqueous solubility. Given that it is very difficult to strongly improve the physico-chemical profile of lead compounds with high logP values without losing activity,[26] a fragment screening was initiated as an alternative[27,28] initially leading to the benzamide **2**.[29] **2** showed mixed agonistic-antagonistic properties. The introduction of a hydroxamic acid motif (**3**) provided a pure antagonistic profile.[29] It is noteworthy that hydroxamic acids are reported as chelating agents[30] and accordingly have been used as inhibitors of various metalloproteins.[31] Furthermore, aromatic hydroxamic acids are described as potential mutagenic agents.[32] In order to overcome these shortcomings and to gain chemical diversity, it was of major interest to discover PqsR antagonist with alternative scaffolds.

In this work, we present the discovery of structurally diverse, low molecular weight PqsR ligands employing surface plasmon resonance (SPR) biosensor experiments. Selected hits displaying sufficient affinity were functionally and thermodynamically characterized. Furthermore, the most promising hit compound **5** was structurally optimized and transformed into the potent PqsR antagonist **37** which was able to reduce the production of HHQ in a PqsH deficient mutant and the major virulence factor pyocyanin in wild-type *P. aeruginosa*.

RESULTS AND DISCUSSION

Chemistry. The top screening hits **4-9** (Figure 2) were commercially available. The synthesis of the thiadiazole and oxadiazole derivatives was achieved by the use of different synthetic routes as described in the following.

Scheme 1. Synthesis of Oxadiazole-2-amine and Thiadiazole-2-amine Derivatives[a]

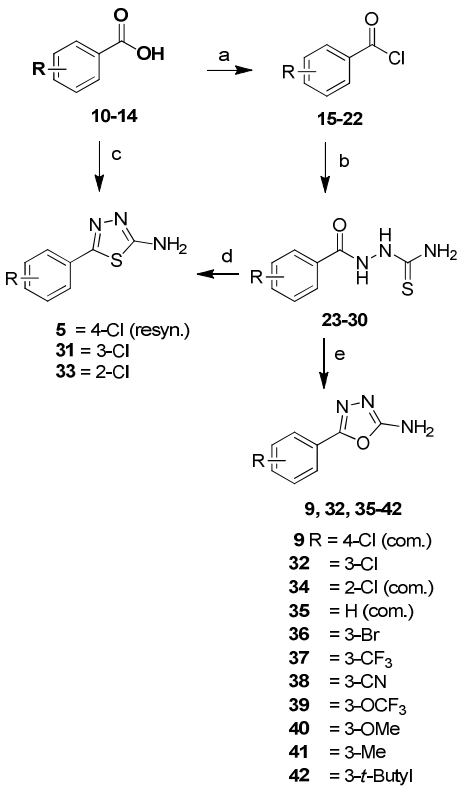

[a] Reagents and Conditions: (a) oxalyl chloride, DMF cat, DCM, reflux; (b) thiosemicarbazide, THF, 0 °C to RT; (c) thiosemicarbazide, $POCl_3$, 80°C; (d) H_2SO_4, RT; (e) 1,3-Dibromo-5,5-dimethylhydantoin, KI, NaOH, 2-propanol, 4 °C.

The synthesis of 1,3,4-oxadiazole-2-amine and 1,3,4-thiadiazole-2-amine derivatives is shown in Scheme 1. Thiadiazoles **5** and **33** were synthesized in a one-step procedure from commercially available benzoic acid derivatives and hydrazinecarbothioamide in $POCl_3$.[33] A classic coupling

reaction of benzoic acid chlorides and hydrazinecarbothioamide afforded the benzoylthiosemicarbazides **23-30**.[34] **31** was obtained by treating the respective benzoylthiosemicarbazide **23** with concentrated sulfuric acid as dehydrating agent.[35] The ring closure which gives the respective 2-amino-1,3,4-oxadiazoles **32** and **35-42** was achieved under mild oxidative conditions using compounds **23-30** and employing 1,3-dibromo-5,5-dimethylhydantoin as primary oxidant in the presence of catalytic amounts of potassium iodide.[34]

Scheme 2. Synthesis of 2-Substituted Oxadiazoles[a]

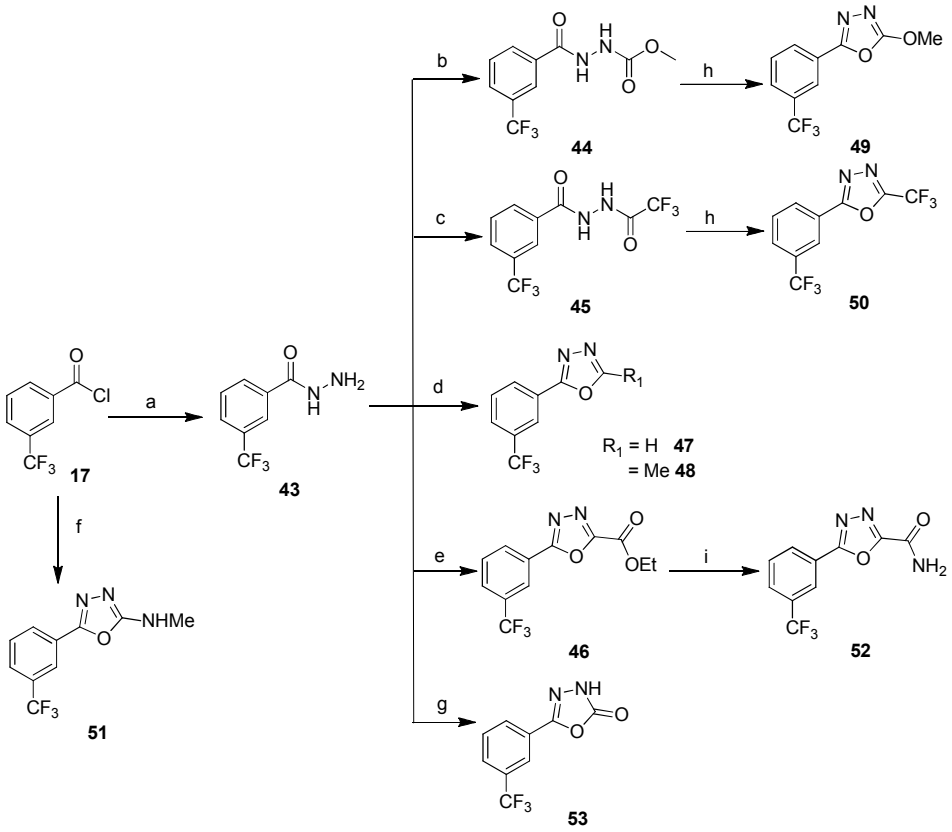

[a] Reagents and Conditions: (a) methanol, Et_3N, RT, then hydrazine hydrate, water, 120 °C; (b) methyl chloroformate, $NaHCO_3$, water, dioxane, 0 °C; (c) trifluoroacetic anhydride, Et_3N, DCM, RT; (d) $R_1C(OEt)_3$, 150 °C; (e) ethyl oxalyl monochloride, Et_3N, DCM, 0 °C then tosyl chloride, RT; (f) *N*-methylhydrazinecarbothioamide, DCM, RT then EDC, 40 °C; (g) carbonyldiimidazole, Et_3N, DCM, RT; (h) Burgess reagent, THF, MW radiation, 100 W, 150 °C; (i) ammonia in methanol, RT.

The synthesis of compounds containing variations in the 2-position of the oxadiazole heterocycle (**47–53**) is summarized in Scheme 2. The precursor 3-(trifluoromethyl)benzohydrazide (**43**) was obtained from the corresponding benzoyl chloride **17** in a two-step procedure. Coupling of **43** with methyl chloroformate and trifluoroacetic anhydride afforded **44** and **45**. Ring-closure was carried out under microwave radiation using Burgess reagent as selective dehydrating agent yielding compounds **49** and **50**.[36] Heating of **43** in triethyl orthoformate or triethyl orthoacetate provided the oxadiazoles **47** and **48**, respectively.[37] **46** was synthesized in a one-pot two-step procedure, following the coupling of **43** with ethyl oxalyl monochloride and ring closure with tosyl chloride.[38] **46** was treated with ammonia in methanol to directly transform the ethyl ester in the corresponding carboxamide **52**.[39] The *N*-methylated analog **51** was obtained in a one-pot two-step protocol: the benzoylchloride was coupled with *N*-methylhydrazinecarbothioamide and ring closure was carried out by employing EDC.[40] Oxadiazol-2-one **53** was prepared by conversion of **43** with carbonyldiimidazole.[41]

Identification of PqsR Ligands by Fragment Screening. The detection and analysis of biomolecular interactions is one of the key issues in the hit identification phase of a drug discovery project. Surface plasmon resonance spectroscopy represents a powerful tool to monitor and characterize binding events in real-time.[42] We have applied this technology to screen a library containing 720 compounds with a molecular weight ranging from 100 to 350 g/mol (for details see SI; Table S2). PqsR was immobilized on the sensor chip surface *via* biotin-streptavidin specific interaction and compounds were initially screened at a single concentration of 100 μM. Approximately 40 binding compounds were selected based on affinity and selectivity against negative control (bovine carbonic anhydrase II). Compounds showing undesirable SPR binding characteristics as described by Giannetti *et al.*[43] were not taken into consideration. These included fragments displaying binding irregularities, fragments with non-typical slow dissociation and compounds producing super-stoichiometric binding responses. The obtained hit rate of 5-6% can be regarded as excellent compared to the screening of more complex structures.[28] The best fragments were further subjected to SPR dose-ranging experiments to accurately determine dissociation constants (K_D values). The five top candidates displayed K_D values below 11 μM (**4**-**8**, Figure 2 and Table 1). To further evaluate binding of the best screening hits we performed SPR competition experiments similar to those described previously.[44] Dose binding experiments with mixtures consisting of various concentrations of either compound **4** or **5** and constant concentrations of PQS showed no overall additivity in the SPR response (SI, Figure S2). Increasing the PQS concentration did not exceed the maximal binding capacity of the chip surface (R_{max}; experimentally determined for the different fragments). These results show that both fragments compete with PQS for binding to PqsR.

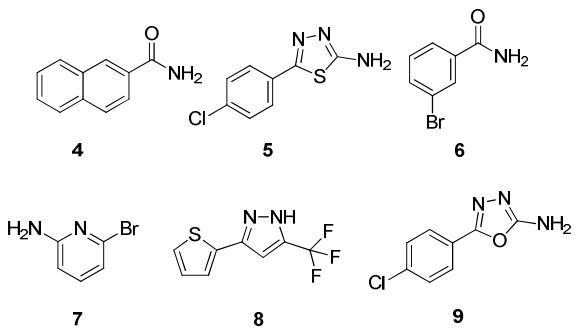

Figure 2: Chemical structures of highest affinity compounds **4-8** and compound **9**

As evaluation of the K_D values alone gives no clear indication of which ligands to select for further progression,[45] the thermodynamic parameters, which allow a more detailed understanding of biomolecular interactions,[46] were determined (Table 1) using isothermal titration calorimetry (ITC).

Table 1: Biophysical characterization of PqsR ligands.[a]

Comp.	$K_{D\,(SPR)}$ [μM][b]	$K_{D\,(ITC)}$ [μM]	ΔG [kcal mol^{-1}]	ΔH [kcal mol^{-1}]	$-T\Delta S$ [kcal mol^{-1}]	LE [kcal mol^{-1}]
2	-	0.9±0.0	-8.3±0.0	-9.7±0.3	1.5±0.3	0.63
4	0.8±0.2	1.8±0.2	-7.9±0.1	-8.6±0.2	0.7±0.2	0.60
5	4.5±0.0	3.7±0.1	-7,4±0.0	-8.2±0.9	0.7±0.9	0.57
6	6.8±3.5	7.6±0.7	-7.0±0.1	-6.9±0.1	0.1±0.1	0.70
7	6.8±3.8	10.0±1.3	-6.8±0.1	-9.3±0.4	2.5±0.4	0.85
8	10.7±6.5	8.5±0.7	-6.9±0.0	-8.6±0.0	1.6±0.1	0.49
9	200-500	-	-	-	-	-
37	-	1.3±0.3	-8.0±0.1	-8.5±0.5	0.4±0.5	0.50
41	-	12.4±1.0	-6.7±0.0	-4.0±0.1	-2.6±0.1	0.51
42	-	3.1±0.6	-7.5±0.1	-7.6±0.0	0.0±0.1	0.47
47	-	6.5±0.5	-7.1±0.0	-9.0±0.5	1.9±0.3	0.47
48	-	12.9±2.4	-6.7±0.1	-3.8±0.2	-2.8±0.3	0.42

[a]SPR measurements and ITC titrations were performed at 20 °C and 25 °C, respectively. Data represent mean ± SD from at least two independent experiments. [b]$K_{D\,(SPR)}$, PQS: 0.21±0.0 μM

The ITC derived K_D values were in good accordance with the ones determined by SPR experiments. The naphthalene-2-carboxamide **4** and the thiadiazole derivative **5** displayed the

highest affinities (Table 1). Analysis of the thermodynamic signatures revealed that **4-8** are enthalpy-driven binders (Table 1) indicating a good non-covalent bond complementarity between the protein site and the compounds.[45] Given that it is harder to improve the ΔH contribution than to improve the ΔS contribution, enthalpy driven binders are usually preferred for further optimization.[45] Moreover, we determined the ratio of Gibb's free binding energy to the number of non-hydrogen atoms termed ligand efficiency (LE) that enables a better comparison of hits with widely differing structures and activities.[47] Compounds **4-8** showed LEs ranging from 0.49 to 0.85 kcal/mol and are above the threshold value of 0.33 kcal/mol, which should be exceeded for an efficient optimization.[47] In order to evaluate the agonistic and antagonistic activities of **4-8**, we examined the PqsR-mediated transcriptional effect in a reporter gene assay by measuring the β-galactosidase activity in *E. coli* the pEAL08-2 plasmid containing the tac_P-*pqsR* and $pqsA_P$-*lacZ* fusion genes (Table 2).[48] *E. coli* was used, as it provides a system to characterize the functionality of PqsR ligands independent of the entire *pqs* system and the low outer membrane permeability[49] characteristic for *P. aeruginosa*. While **6-8** showed no or only weak antagonistic activity, compounds **4** and **5** exhibited marked antagonistic properties. In contrast to compound **4**, compound **5** provided only moderate agonistic activity. Overall, the screening process afforded thiadiazole **5** which combines a remarkably high affinity with regard to its low molecular weight with superior functional properties in the *E. coli* reporter gene assay and was therefore selected for further optimization.

Fragment Optimization. Another hit compound sharing a high degree of similarity with **5**, compound **9** (Figure 2), which had shown lower affinity in the SPR screen, but pure antagonistic activity (Table 2) was included in the optimization strategy (Figure 3).

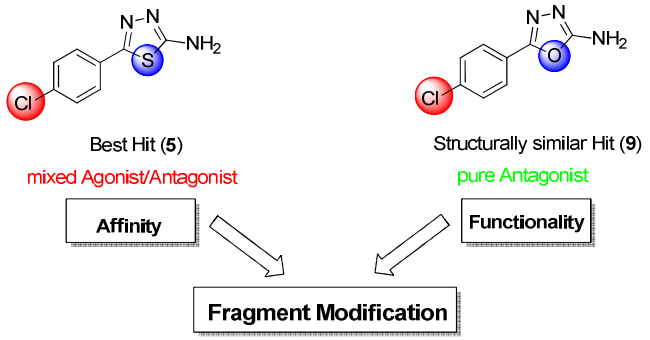

Figure 3: Fragment modification strategy

In the first modification step the position of the Cl substituent was shifted into the *meta* and *ortho* position (Table 2), as we had observed that the antagonistic properties in the quinolone class of PqsR antagonists strongly depended on the position of the aromatic substituents.[25] The compounds with Cl in *meta* position showed an opposed functional profile in case of both heterocycles: the thiadiazole **31** displayed pure agonistic properties, while the oxadiazole **32** turned out to be a pure antagonist. The Cl substituent in *ortho* position (**33**, **34**) led to a moderate agonistic activity without antagonistic properties for both heterocycles.

Compound **32** was used for further optimization. The Cl group was exchanged for substituents providing different electronic properties (**35-42**, Table 2). Omitting the Cl substituent (**35**) led to a moderate agonistic activity. The bioisosteric exchange of Cl for electron-withdrawing moieties in *meta* position (**36-39**) resulted in pure antagonists with the Br compound **36** and the CF_3 derivative **37** as the most potent ones (EC_{50} 7.5 µM). Interestingly, in the class of HHQ derived antagonist a CF_3 substituted quinolone also showed the strongest antagonistic properties.[25] The introduction of a methoxy group (**40**) was accompanied by a complete loss of activity. In contrast, the introduction of a methyl substituent resulted in a partial antagonist (**41**, SI, Figure S5). In the case of the benzamide scaffold reported by Klein *et al*. (**2**, Figure 1) the exchange of Cl for *tert*-butyl resulted in an increased affinity due to an enthalpic gain.[29] Assuming a similar

binding mode of **2** and **37** (discussed in detail below) this structural modification was deemed to have a similar effect in the oxadiazole class. Compound **42,** however, showed a slightly reduced affinity according to ITC analysis (Table 1) and more importantly a diminished antagonistic activity. Overall, **37** showing a favorable logP of 2.12 (ACD Perspecta 14.0.0 consenus logP) and a better aqueous solubility compared to **36** emerged as the most promising compound. Accordingly, **37** was tested in the *P. aeruginosa* reporter gene assay. As the outer membrane is much less permeable in *P. aeruginosa*[49] the observed antagonistic activity being only 5-fold reduced (EC_{50}s: 7.5 µM in *E. coli*, 38.5 µM in *P. aeruginosa*; SI Figure S6) was remarkably high.

Table 2: Agonistic and antagonistic activities of PqsR ligands[a]

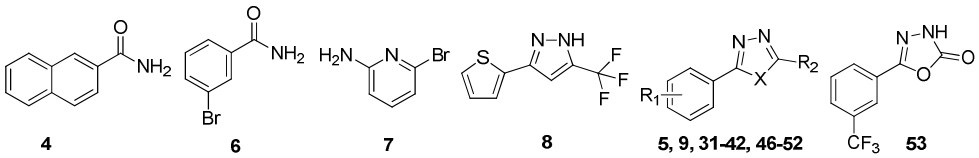

Compd.	Pos	X	R_1	R_2	Agonistic activity [%]	Antagonistic activity [%]	*EC50*[b] [µM]
4	-	-	-	NH_2	52±12	41±12	-
5	4	S	Cl	NH_2	28±1	43±16	-
6	-	-	-	NH_2	n.a.	n.i.	-
7	-	-	-	NH_2	n.a.	22±17	-
8	-	-	-	NH_2	n.a.	n.i.	-
9	4	O	Cl	NH_2	n.a.	40±9	-
31	3	S	Cl	NH_2	105±11	n.i.	-
32	3	O	Cl	NH_2	n.a.	76±12	26.7
33	2	S	Cl	NH_2	48±1	n.i.	-
34	2	O	Cl	NH_2	22±5	n.i.	-
35	3	O	H	NH_2	28±3	n.i.	-
36	3	O	Br	NH_2	n.a.	105±6	7.5
37	3	O	CF_3	NH_2	n.a.	111±13	7.5
38	3	O	CN	NH_2	n.a.	84±1	17.8
39	3	O	OCF_3	NH_2	n.a.	69±6	46.5
40	3	O	OMe	NH_2	n.a.	n.i.	-
41	3	O	Me	NH_2	n.a	55±20	57.8[c]
42	3	O	t-Butyl	NH_2	n.a.	42±11	-
47	3	O	CF_3	H	n.a.	49±22	101.2
48	3	O	CF_3	Me	n.a.	n.i.	-
49	3	O	CF_3	OMe	n.a.	n.i.	-
50	3	O	CF_3	CF_3	n.a.	n.i.	-
51	3	O	CF_3	NHMe	n.a.	n.i.	-
52	3	O	CF_3	$CONH_2$	39±6	n.i.	-
53	-	-	-	-	41±4	n.i.	-

[a]Agonistic and Antagonistic properties were evaluated in an *E. coli* reporter gene assay. Agonistic activity was determined by measuring the PqsR stimulation induced by 100 µM of the test compound compared to 50 nM PQS (= 100%); n.a. = no agonism (agonistic activity ≤ 20%). Antagonistic activity was determined by measuring the inhibition of the PqsR stimulation induced by 50 nM PQS in the presence of 100 µM test compound (full inhibition = 100%); n.i. = no inhibition (antagonistic activity ≤ 20%). Mean values of at least two independent experiments with n = 4. [b]Concentration of the half maximal antagonistic activity. Mean values of at least two independent experiments with compounds tested in at least 6 different concentrations and n = 4. [c]partial antagonist

Characterization of Fragment Binding Mode. Despite many efforts,[50,51] the 3D structure of the PqsR protein is not available. The amino acids Q194 and F221 are located within the LBD of PqsR and are potential partners for non-covalent interactions.[29] We could clearly show that Q194 and F221 are involved in the binding of benzamide **2** employing site-directed mutagenesis in combination with ITC analysis.[29] Accordingly, the optimized compound **37** and the screening hit naphthalene-2-carboxamid **4** showing highest affinity were evaluated for their binding to the Q194A and F221A PqsR mutants by ITC (Table 3).

Table 3: Effect of site-directed mutations on the thermodynamic parameters of PqsR ligands.

	Q194A			F221A		
Ligand	$\Delta\Delta G$ [kcal mol^{-1}]	$\Delta\Delta H$ [kcal mol^{-1}]	$-T\Delta\Delta S$ [kcal mol^{-1}]	$\Delta\Delta G$ [kcal mol^{-1}]	$\Delta\Delta H$ [kcal mol^{-1}]	$-T\Delta\Delta S$ [kcal mol^{-1}]
2	-1.3±0*	-4.4±0.3*	3.1±0.3*	-1.0±0.1*	-7.6±0.3*	6.6±0.4*
4	-1.1±0.1*	-3.2±0.2*	2.1±0.2*	-0.4±0.1*	-7.1±0.2*	6.7±0.2*
37	-0.6±0.1*	-0.3±0.6	-0.3±0.7	-0.6±0.1*	-7.1±0.5*	6.5±0.6*

$\Delta\Delta G$, $\Delta\Delta H$, and $-T\Delta\Delta S$ are $\Delta G_{WT} - \Delta G_{mutant}$, $\Delta H_{WT} - \Delta H_{mutant}$, and $-T(\Delta S_{WT} - \Delta S_{mutant})$, respectively. Negative values indicate a loss, positive values a gain compared to wild-type. Errors indicate SD calculated *via* Gaussian error propagation. Significance: effect of the point mutation on the thermodynamic parameters of ligand binding compared to the wild-type. * $p < 0.003$; * $p < 0.05$.

Comparing the thermodynamic signatures of **4** binding to Q194A mutant and wild-type PqsR a loss in ΔH of 3.2 kcal/mol was observed. Given that a well-placed H-bond makes a favorable enthalpic contribution in a range from 4 to 5 kcal/mol,[52] this value indicates the presence of a weak H-bond between **4** and Gln194. The enthalpic contribution of **4** binding to the F221A mutant was significantly reduced compared to the wild-type ($\Delta\Delta H$ = -7.1 kcal/mol). F221 might be involved in a π-π interaction with the naphthalene core of **4**. However, theoretical investigations revealed an interaction energy of only 4.0 to 4.2 kcal/mol for the benzene-

naphthalene complex.[53] In all cases the loss in enthalpy is partly compensated by a gain in entropy. This might be due to a higher conformational flexibility of the complex in the absence of specific non-covalent interactions. Overall, the measured data indicate that napthalene-2-carboxamide **4** adopts the same binding mode as the benzamide **2**.

In contrast, there was no significant difference in the enthalpic contribution observed for the oxadiazole **37** when binding to Q194A mutant and wild-type PqsR. This indicates that the side-chain of Gln194 is not directly involved in the binding of **37**. As observed for **4**, the binding of **37** was also affected by the F221A mutation ($\Delta\Delta H$ = -7.1 kcal/mol). The phenyl moiety of **37** might be involved in a π-stacking interaction with F221. Overall, these data lead to the conclusion that aromatic carboxamides **2** and **4** as well as the oxadiazole **37** interact with different amino acids within the LBD by adopting different binding modes. ITC analysis was applied to analyze whether both fragments bind to the same site. PqsR was saturated with an excess of **2** and **37** was titrated subsequently into the same solution (Figure 4a). No additional heat release was detected which gives strong evidence that both compounds compete for binding to PqsR. Additionally, the *vice versa* experiment was performed to exclude that the binding of **2** induces a conformational change which hinders the binding of **37**. This experiment led to the same result (SI Figure S4) confirming that both fragments bind to the same site. In order to further validate the competitive binding (**2**, **37**) we applied NMR INPHARMA experiments.[54] This technique allows to detect protein-mediated interligand NOEs, if both compounds bind competitively to the same site of the protein. When we conducted a 2D NOESY experiment of a mixture of **2** and **37** in the presence of PqsR, clear interligand NOEs between the tert-butyl group of **2** and the phenyl ring of **37** were observed (Figure 4b, upper panel). Additionally, weaker interligand NOEs between the two phenyl moieties of **2** and **37** were detected (Figure 4b, lower

panel). These findings corroborated our ITC data that both ligands bind competitively to the same site of PqsR. Given that both fragments interact with F221 and compete with PQS as shown for the structural analogs **4** and **5** in SPR competition experiments, we conclude that **2** and **37** have overlapping binding sites within the LBD.

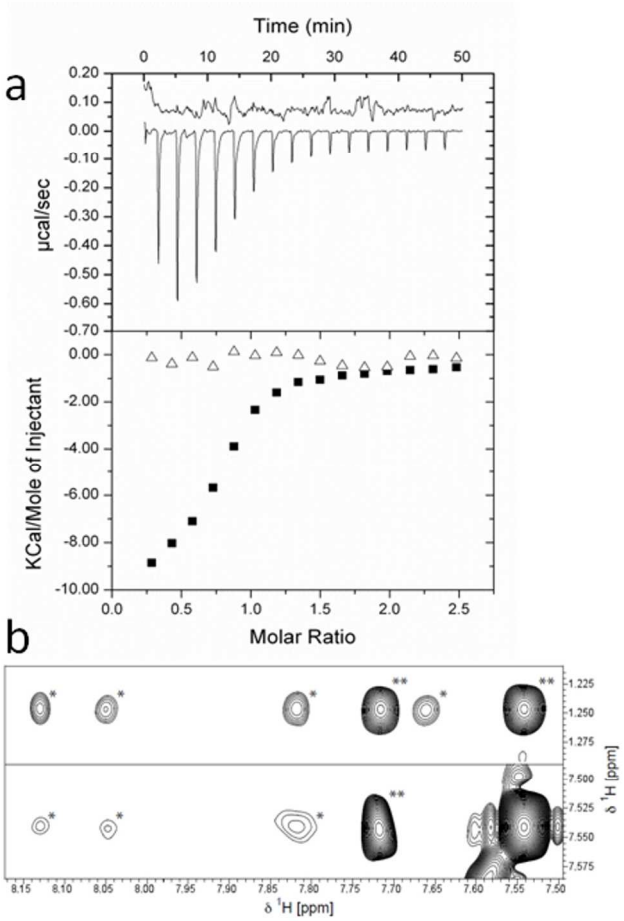

Figure 4. Competitive binding of **2** and **37** to PqsR (a) Raw ITC data (top) and integrated normalized data (bottom) for titrations of 43 µM PqsR with 500 µM **37** in the absence of **2** (■) and in the presence of 500 µM compound **2** (Δ). (b) NOESY spectrum of a mixture of 500 µM **2** and 400 µM **37** in the presence of 10 µM PqsR; interligand NOEs between the tert-butyl moiety of **2** and the phenyl ring of **37** (top), between the two phenyl rings (bottom); (*) indicates interligand INPHARMA NOEs mediated by PqsR; (**) indicates intramolecular transferred NOEs. Signals marked with (*) or (**) were not detected in a control experiment recorded under identical conditions in the absence of PqsR.

Biophysically Guided Structural Modifications. Structural modifications of **37** in combination with thermodynamic analysis were performed to evaluate the relative contributions of the different functional groups. The CF_3 moiety was replaced by a methyl group and the thermodynamic signature of the resulting compound **41** was compared to that of **37** (Figure 5).

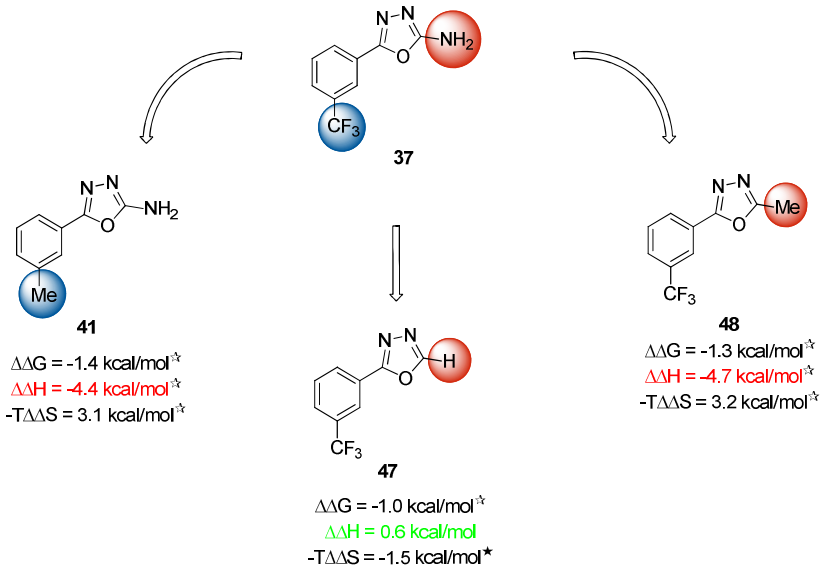

Figure 5. Relative thermodynamic contributions of functional groups. Negative values indicate a loss; positive values a gain compared to compound **37**; $^{☆}p < 0.003$; $^{★}p < 0.05$

Compound **41** showed a reduced affinity for PqsR compared to **37** (Table 1), which was due to a significant loss in ΔH of 4.4 kcal/mol (Figure 5). This corroborates the proposed π-stacking between F221 and the phenyl moiety of the oxadiazole **37** as electron-withdrawing groups like CF_3 can intensify such interactions either through enhanced electrostatic[55,56] or direct effects of the substituents.[57] Considering the loss in enthalpy that is caused by the F221A mutation (7.1 kcal/mol) and the loss in enthalpy that is due to the exchange of the CF_3 by CH_3 (4.4 kcal/mol), the enthalpic contribution of a possible π-π interaction between **37** and Phe221 might be 2.7

kcal/mol. Remarkably, this is consistent with the binding energy of the gas-phase benzene dimer ranging from 2.0 to 3.0 kcal/mol.[58]

The thermodynamic profile of compound **37** binding to Q194A suggested that the amino group of **37** does not make an H-bond with the polar side-chain of Gln194. To investigate whether the amino group is involved in the formation of an H-bond with polar backbone atoms or other side-chains in the LBD of PqsR it was replaced by hydrogen. The binding affinity of the resulting compound **47** was reduced (Table 1). The same tendency was observed for the functional properties (Table 2). But even more interesting, there was no significant difference in the enthalpic contributions (Figure 5). These findings initially led us to the conclusion that the amino group is not involved in a specific non-covalent interaction (e.g. H-bond) with PqsR. Hence, we decided to replace the amino function for apolar moieties with different electronic properties like methyl (**48**), methoxy (**49**) and CF_3 (**50**) in order to overcome the enthalpy penalty associated with desolvation of the polar amino group.[52] In contrast to our assumption, compound **48** displayed a reduced affinity toward PqsR (Table 1), which results from a significant decrease in ΔH of 4.7 kcal/mol (Figure 5) typical for a loss of a well-placed H-bond.[52] Furthermore, these modifications (**48-50**) completely abolished the antagonistic activity (Table 2). These findings led us reconsider our hypothesis of a non-interacting amino function: the C-H bond in 2-position of the 1,3,4-oxadiazole (**47**) is highly polarized and can interact through a non-classical hydrogen bond.[59] In our case such an interaction could be mediated by a water molecule that is displaced in the presence of an amino function (**37**). This explanation is sustained by the loss in entropy (-1.5 kcal/mol) due to the exchange of NH_2 by H. Theoretical investigations revealed an interaction energy for highly similar 5-membered heterocycles like oxazoles and isoxazoles in the range of

3.0 to 3.5 kcal/mol.[59] Such an interaction might compensate the loss in enthalpy by omitting the amino group.

In order to evaluate whether both hydrogen atoms of the amino substituent (**37**) are involved in ligand-receptor interaction we synthesized the *N*-methylated analogue **51**. The latter showed no antagonistic activity (Table 2) as did the carboxamide (**52**) and oxadiazol-2-on (**53**) indicating that the amino group is essential for full antagonistic activity even if the exact function in the ligand-receptor interaction remains speculative.

Effects on alkylquinolone signaling and virulence factor pyocyanin formation in *P. aeruginosa.* Following our strategy of inhibiting *P. aeruginosa* pathogenicity, we evaluated the effect of different oxadiazole derivatives on the production of alkylquinolones and the major virulence factor pyocyanin in the highly virulent clinical isolate *P. aeruginosa* PA14. The activation of PqsR upregulates the *pqsABCD(E)* operon which is essential for HHQ and PQS biosynthesis.[16,19,20] Furthermore, PQS is reported to influence biofilm shape.[21] Accordingly, we examined the effect of **37** on extracellular levels of PQS in wild-type *P. aeruginosa*. As we reported for the HHQ derived antagonist[25] no remarkable reduction of PQS levels was observed (data not shown). We assumed that the autoinductive effect of high intrinsic PQS levels ranging from 30 to 60 μM in the culture supernatant might compensate the antagonistic activity of **37**. Therefore, we further investigated the effect of compound **37** on HHQ formation in the absence of PQS.[17] We employed a *P. aeruginosa* isogenic strain lacking PqsH, a monooxygenase catalyzing the conversion of HHQ to PQS.[19,20] Interestingly, we observed a reduction of extracellular HHQ (42±0% at 250 μM of **37**). The level of HQNO (2-heptyl-4-hydroxy quinoline-*N*-oxide), another alkylquinolone under the control of PqsR,[20] was also clearly decreased (43±3% at 250 μM of **37**). The reduction of both alkylquinolones demonstrates that

PqsR antagonists block the QS system in *P. aeruginosa*. Future experiments will extend the fragment structure aiming at antagonists with improved affinity. Such compounds would hopefully disrupt the self-inductive effect of high intrinsic PQS levels and potentially affect biofilm shape in wild-type *P. aeruginosa*.

The biological effects on the major virulence factor pyocyanin were examined subsequently. Pyocyanin is a redox-active secondary metabolite released by *P. aeruginosa* that plays a critical role during acute infections by provoking oxidative stress and inflammatory responses in host cell tissue.[60] Biological studies indicate a connection between the PQS system and pyocyanin production,[18,61] supported by the fact that a PqsR deficient mutant (*pqsR*$^-$) is incapable to produce pyocyanin.[20,62] Analogously, the HHQ derived antagonist **1**[25] and the hydroxamic acid **3**[29] diminish pyocyanin in *P. aeruginosa*. The PqsR antagonist **37** likewise clearly reduced the pyocyanin level (46±9% at 250 µM). The weaker antagonists **38** and **41** showed a moderate or only little reduction, respectively (32±3% at 250 µM of **38**; 18±3% at 250 µM of **41**). In contrast the inactive compound **40** showed no effect. The correlation of these data with the antagonistic properties indicates that the reduction of pyocyanin is caused by PqsR antagonism. A growth curve of *P. aeruginosa* incubated with **37** confirmed that the observed effects are not due to an antibacterial activity of the compound (SI, Figure S6). While in the absence of functional PqsR (*pqsR*$^-$) no significant levels of pyocyanin and PQS were detected,[20] our results show that in the presence of weaker antagonists pyocyanin production is more sensitive to PqsR antagonism than PQS biosynthesis. This finding might facilitate a more detailed understanding of the underlying mechanisms. Overall these results demonstrate that the interference with the PQS system by the oxadiazole type antagonists is a suitable approach to reduce *P. aeruginosa* pathogenicity.

CONCLUSION

Considering the hydrophobic character of the natural effectors HHQ and PQS, the LBD of PqsR is expected to be a mainly lipophilic pocket. This renders the transcriptional regulator PqsR a quite challenging drug target. Nevertheless, we identified chemically diverse PqsR ligands by employing an SPR fragment screening. The thermodynamic profiles of the top five hit compounds were evaluated using ITC methodology. The discovered hits showed enthalpy driven binding and excellent LEs. Furthermore, the functional properties of the best fragments were analyzed in a ß-galactosidase reporter gene assay as an additional guidepost for hit selection. The thiadiazole-2-amine derivative **5** displayed a mixed agonistic/antagonistic profile and was chosen as starting point for structural modification. A functionality-guided optimization process afforded the pure antagonist **37** showing improved affinity and potency with consistently high LE (**5**, LE = 0.57 kcal/mol *vs.* **37**, LE = 0.50 kcal/mol). In contrast to the HHQ derived antagonists (for example **1**, Figure 1), **37** showed a more favorable logP and higher aqueous solubility. The 2-amino-1,3,4-oxadiazole moiety present in the optimized ligand **37** has not been reported as a chelating agent for metal ions, contrary to the hydroxamic acid motif of fragment **3** (Figure 1). Furthermore, an *in-silico* toxicology prediction (Derek Nexus, Version 2.0.3.201206121715) of compound **37** revealed no safety issues.[63] Taken together these data emphasize the high potential of the optimized fragment **37**.

To shed light on the binding mode of different fragment classes, site-directed mutagenesis in combination with thermodynamic analysis was applied. The oxadiazole **37** and the carboxamides **2** and **4** bind competitively to PqsR but do not cover exactly the same space in the LBD. This provides the potential for hit-to-lead optimization using fragment growing strategies. Additionally, structural modifications of **37** together with calorimetric evaluation were

performed to evaluate the relative importance of the functional groups in order to guide future optimization strategies. Furthermore, compound **37** is able to reduce the virulence factor pyocyanin in wild-type *P. aeruginosa* without affecting bacterial growth. Thus, the identified PqsR antagonists represent an interesting starting point for the development of novel anti-infectives.

Future experiments will aim at merging the best features of the different fragments to develop drug-like molecules which may provide novel therapeutic options to counter the burden of *P. aeruginosa* infections.

EXPERIMENTAL SECTION

Surface Plasmon Resonance. SPR binding studies were performed using a Biacore T100 instrument optical biosensor (GE Healthcare). CSIRO fragment library collection consisted of 720 compounds with a molecular weight range of 100 to 350 Da. The expression, purification and minimal biotinylation of H_6SUMO-PqsR^{C87} as well as the immobilization onto the streptavidin chip surface and is described in detail in the Supporting Information.

SPR Library Screening. 10 mM DMSO stock solutions of compounds were diluted in 1.05 x DMSO free screening buffer (52.5 mM HEPES, pH 7.4, 157.5 mM NaCl, 0.0525% Tween-20 (v/v)) to 500 μM. Final ligand concentrations (100 μM) were achieved by diluting 1:5 (v/v) in the instrument running buffer (50 mM HEPES, pH 7.4, 150 mM NaCl, 0.05% Tween-20 (v/v) and 5% DMSO (v/v)). Two separate fragment screens were performed each time screening 360 fragments against protein targets immobilized on chips I and II. Fragment solutions (100 μM) were injected over the protein sensor surface for 30 s at 60 μL/min at 4 °C. After every 120 injections, a positive control compound (PQS in the first 360 compound screen and fragment **4** in the second screen) was injected for control binding purposes. Regeneration of the surfaces between subsequent binding experiments was achieved by washing the surface at 60 μL/min for 30 s with the instrument running buffer as well as by using a "carry-over injection" of running buffer at 40 μL/min for further 30 s. To determine binding affinity, candidate hit fragments were analyzed using dosage experiments. Fresh 100 mM DMSO fragment solutions were diluted directly into instrument running buffer to a final concentration of 81 μM and then diluted 3-fold down to 1 μM aiming for a 5-point concentration series range. Each compound was injected for 30 s association- and 60 s dissociation time at 20 °C at a constant flow rate of 60 μL/min.

Scrubber 2 (www.biologic.com.au) and Microsoft Excel software packages were utilized for data processing and analysis. Using Scrubber software, SPR signals were referenced against the blank surface (streptavidin + D-biotin) and further corrected for DMSO refractive index change as previously described.[64] A normalization scheme of Giannetti *et al*.[43] was applied to the processed data based on the maximal binding response (R_{max}) that has been determined from experiments with the control compound (initially PQS and later fragment **4**). For the initial ranking of the best hits, the K_D values were estimated using equation derived from the Langmuir adsorption isotherm (1):

$$K_D = \frac{R_{max}*C}{R} - C \quad (1)$$

R_{max}, R, and C correspond to the normalized saturation response of the compound, the normalized response of the test compound, and the concentration of the test solution, respectively.

To determine binding affinities (K_D) from dosage experiments, binding responses at equilibrium were fit to a 1:1 steady state affinity model available within Scrubber. As described above, normalized saturation response (R_{max}), derived using reference compound(s), was applied to response curves obtained with fragment hits at non-saturating concentration. Equilibrium isotherm containing the assumed R_{max} was used to determine K_D values (SI, Figure S1).

Isothermal titration calorimetry ITC titrations were carried out as previously reported[29] and a detailed protocol as well as representative titration curves are included in the Supporting Information.

INPHARMA NMR Experiments To detect interligand NOEs, 10 μM H_6SUMO-PqsR^{C87} was mixed with 500 μM **2** and 400 μM **37** in PBS buffer (50 mM potassium phosphate, pH 7.4, 150 mM NaCl, 5% DMSO-d_6 (v/v), 5 % D_2O (v/v)). Spectra were acquired at 25 °C on a 700 MHz Bruker Avance III spectrometer equipped with a cryoprobe. Two-dimensional NOESY spectra were recorded with a mixing time of 600 ms, 16 scans for each of 400 complex points in the indirect dimension and 512 complex points in the direct dimension, a sweep width of 9 ppm and a recycle delay of 1.5 sec. Dephasing of water signals was achieved by a WATERGATE sequence. A control experiment under identical conditions without H_6SUMO-PqsR^{C87} was carried out. Data were processed using Bruker TOPSPIN 3.1 software using squared sine bell functions and zero filling to 2048 and 1024 complex points in the direct and indirect dimension, respectively, for apodization.

Reporter Gene Assay in *E. coli*. The ability of the compounds to either stimulate or antagonize the PqsR-dependent transcription was analysed as previously described[25] using a β-galactosidase reporter gene assay in *E. coli* expressing PqsR with some modifications to enable a higher throughput.[65] Briefly, a culture of *E. coli* DH5α cells containing the plasmid pEAL08-2[48] which encodes PqsR under the control of the *tac* promoter and the β-galactosidase reporter gene *lacZ* controlled by the *pqsA* promoter were co incubated with test compound. Antagonistic effects of compounds were assayed in the presence of 50 nM PQS. After incubation galactosidase activity was measured photometrically using POLARstar Omega (BMG Labtech) and expressed as ratio of controls. For the determination of EC_{50} value, compounds were tested at least in six different concentrations. The given data represent mean of at least two experiments

with n = 4. The log (inhibitor) vs. response model (Prism 5.0) was applied for nonlinear regression and determination of EC_{50}-values.

Reporter Gene Assay in *P. aeruginosa.* In order to evaluate the antagonistic properties of compound **37**, the PqsR-dependent transcription was evaluated as previously described[25] using a β-galactosidase reporter gene assay system[48] in *P. aeruginosa*. In brief, a *P. aeruginosa* PA14 strain carrying a nonfunctional *pqsA* gene was used to eliminate intrinsic HHQ and PQS production. A culture of *P.aeruginosa* PA14*ΔpqsA* cells containing the plasmid pEAL08-2[48] were co incubated with **37** and 50 nM PQS. After incubation galactosidase activity was measured photometrically using POLARstar Omega (BMG Labtech) and expressed as ratio of controls. For the determination of EC_{50} value, **37** was tested at nine different concentrations. The given data represent mean of two experiments with n = 4. The log (inhibitor) vs. response model (Prism 5.0) was applied for nonlinear regression and determination of EC_{50}-values.

Pyocyanin Assay. Pyocyanin produced by *P. aeruginosa* PA14 was determined as described previously[66] according to the method of Essar *et al*.[67] In short, cultures inoculated with a starting OD_{600} of 0.02 were grown in the presence of inhibitors or DMSO as a control in PPGAS medium at 37 °C, 200 rpm and a humidity of 75% for 16 h. For pyocyanin determination, cultures were extracted with chloroform and re-extracted with 0.2 M HCl. The OD_{520} was determined using FLUOstar Omega (BMG Labtech) and normalized to cell growth measured as OD_{600}. For each sample, cultivation and extraction were performed in triplicates.

Determination of Extracellular HHQ and HQNO Levels. Extracellular levels of HHQ and HQNO were determined according to the methods of Lépine *et al.*[68,69] with some modifications: Briefly, cultures of *P. aeruginosa* PA14Δ*pqsH* mutant were inoculated with a starting OD_{600} of 0.02 and grown in LB medium in the presence of DMSO as a control or DMSO solutions of inhibitors at 37 °C, 200 rpm and a humidity of 75 % for 17 h. For HHQ and HQNO analysis, 500 µl of bacterial cultures were supplemented with 50 µL of a 10 µM methanolic solution of the internal standard (IS) 5,6,7,8-tetradeutero-2-heptyl-4(1*H*)-quinolone (HHQ-d_4) and extracted with 1 mL of ethyl acetate by vigorous shaking. After centrifugation (14, 000 rpm, 12 min), 400 µL of the organic phase were evaporated to dryness in LC glass vials and dissolved in methanol. For each sample, cultivation and extraction were performed in triplicates. UHPLC-MS/MS analysis was performed as described in detail by Storz *et al.*[67] The following ions were monitored (mother ion [m/z], product ion [m/z], scan time [s], scan width [m/z], collision energy [V], tube lens offset [V]): HHQ: 244, 159, 0.5, 0.01, 30, 106; HQNO: 260, 159, 0.1, 0.01, 25, 88; HHQ-*d4* (IS): 248, 163, 0.1, 0.01, 32, 113. Xcalibur software was used for data acquisition and quantification with the use of a calibration curve relative to the area of the IS.

Chemical and Analytical Methods. ^{1}H and ^{13}C NMR spectra were recorded on a Bruker DRX-500 instrument. Chemical shifts are given in parts per million (ppm), and referenced against the residual solvent peak. Coupling constants (*J*) are given in hertz. Purity control of final compounds was carried out using a SpectraSystems-MSQ LCMS system (Thermo Fisher Scientific) consisting of a pump, an autosampler, VWD detector and a ESI quadrupole mass spectrometer by determination of the relative peak area in the UV trace. Purities were greater than 95%. Mass spectrometry was performed on an MSQ electro spray mass spectrometer

(Thermo Fisher Scientific). High resolution mass spectra were recorded on a maXis 4G hr-ToF mass spectrometer (Bruker Daltonics). Reagents were used as obtained from commercial suppliers without further purification. Procedures were not optimized regarding yield. Microwave assisted synthesis was carried out in a Discover microwave synthesis system (CEM). Column chromatography was performed using the automated flash chromatography system Combiflash Companion (Teledyne Isco) equipped with RediSepRf silica columns. Final products were dried under reduced pressure at 40 °C or in high vacuum. Melting points were determined using the melting point apparatus SMP3 (Stuart Scientific) and are uncorrected.

Screening hits **4**-**8** were obtained from the CSIRO fragment library and used for biological studies. **5** was resynthesized as described below. **2** was purchased from Alfa Aesar; **9**, **34** and **35** were purchased from Sigma Aldrich.

Preparation of Thiodiazole-2-amines (General Procedure 1)[33] Benzoic acid (1 mmol) and hydrazinecarbothioamide (1 mmol) were filled into a sealed reaction vial. Phosphorus oxychloride (4 mmol) was added while cooling on an ice bath. Afterwards, the mixture was heated to 80 °C for 2.5 h in a metal block. Built up pressure was released every hour. The reaction mixture was poured into water at 0 °C and stirred vigorously for 30 min. The mixture was alkalized using a 10 M solution of KOH. The resulting suspension was extracted with ethyl acetate (3 times). The combined organic layers were washed with brine, dried over $MgSO_4$, and concentrated to yield the expected 5-phenyl-[1,3,4]-thiadiazole-2-amine.

Preparation of benzoylthiosemicarbazides (General Procedure 2)[34] Hydrazinecarbothioamide (3 mmol) and THF (5 ml) were filled into a three necked round bottom flask. Benzoyl chloride (1 mmol) was added through a dropping funnel at 0 °C (ice-bath). The mixture was stirred at RT under nitrogen atmosphere for 24 h. The mixture was quenched by the

addition of water and alkalized using a saturated aqueous solution of $NaHCO_3$. Afterwards, THF was evaporated under reduced pressure until precipitation of a solid. The suspension was filtered and the resulting cake was washed with water to afford the expected benzoylthiosemicarbazide.

Preparation of Oxadiazole-2-amines (General Procedure 3)[34] Benzoylthiosemicarbazide (1 mmol) was filled into a three necked flask and suspended in IPA (7 ml). The suspension was mixed with a solution of potassium iodide (0.3 mmol) in water (0.5 mL). The reaction was cooled to 0 °C on an ice-bath and a 5 M solution of NaOH (1.5 mmol) was added. Dibromodimethylhydantoine (0.75 mmol) dissolved in ACN (3 ml) was added through a dropping funnel over 1 h while maintaining the temperature below 10 °C. Afterwards, the reaction was aged for 1 h below 10 °C. The reaction mixture was quenched using $NaHSO_3$ sat. (0.25 mL) and water was added. The pH was adjusted to >12 using a saturated solution of $NaHCO_3$. The suspension was filtered and low boiling solvents were removed from the filtrate under reduced pressure to give a precipitate. The suspension was filtered and the cake rinsed with water and IPA to give the 5-phenyl-[1,3,4]-oxadiazole-2-amine.

5-(4-Chlorophenyl)-1,3,4-thiadiazol-2-amine (5) was prepared according to General Procedure 1 starting from 4-chlorobenzoic acid (**10**, 1.00 g, 6.39 mmol) and hydrazinecarbothioamide (0.582 g, 6.39 mmol). The obtained solid was recrystallized from ethanol to give the pure product as white needles (0.51 g, 2.44 mmol, 38% yield). ^{1}H NMR (500 MHz, DMSO-d_6) δ ppm 7.47 (s, 2 H), 7.50 - 7.55 (m, 2 H), 7.73 - 7.79 (m, 2 H); ^{13}C NMR (126 MHz, DMSO-d_6) δ ppm 127.88 (2 C), 129.13 (2 C), 129.82, 133.92, 155.08, 168.81; mp 231-232 °C; LC-MS (ESI): *m/z*: 252.88 $(M+H+CH3CN)^+$; 98%

5-(3-Chlorophenyl)-1,3,4-thiadiazol-2-amine (31)[35] 2-(3-chlorobenzoyl)hydrazinecarbothiamide (**23**, 0.50 g, 2.18 mmol) was dissolved in sulfuric acid (3 ml). The mixture was stirred for 2 h at RT. The reaction mixture was slowly poured into water and basified using ammonia solution 20% while cooling on an ice bath. The resulting suspension was filtered and the resulting cake was washed with water to give the pure product as a white solid (0.37 g, 1.75 mmol, 80% yield). ^{1}H NMR (500 MHz, DMSO-d_6) δ ppm 7.47 - 7.50 (m, 2 H), 7.52 (s, 2 H), 7.66 - 7.72 (m, 1 H), 7.77 - 7.81 (m, 1 H); ^{13}C NMR (126 MHz, DMSO-d6) δ ppm 125.07, 125.39, 129.23, 131.04, 132.87, 133.78, 154.72, 169.05; mp 214-218°C; MS (ESI): m/z: 212.00 $(M+H)^+$, 252.82 $(M+H+CH_3CN)^+$; 96%.

5-(3-Chlorophenyl)-1,3,4-oxadiazol-2-amine (32) was prepared according to General Procedure 3 starting from 2-(3-(chloro)benzoyl)hydrazinecarbothioamide (**23**, 0.500 g, 2.18 mmol). The titled product was obtained as yellow solid (0.199 g, 1.02 mmol, 47% yield). ^{1}H NMR (500 MHz, DMSO-d_6) δ ppm 7.34 (s, 2 H) 7.56 - 7.58 (m, 2 H) 7.71 - 7.77 (m, 2 H); ^{13}C NMR (126 MHz, DMSO-d_6) δ ppm 123.60, 124.43, 126.23, 130.10, 131.31, 133.81, 156.12, 164.08; mp 251-255°C; MS (ESI): *m/z*: 236.81 $(M+H+CH_3CN)^+$; 95%.

5-(2-Chlorophenyl)-1,3,4-thiadiazol-2-amine (33) was prepared according to General Procedure 1 starting from 2-chlorobenzoic acid (**12**, 1.00 g, 6.39 mmol) and hydrazinecarbothioamide (0.582 g, 6.39 mmol). The obtained solid was adsorbed on silica gel and purified by flash-chromatography using a gradient of hexane/ethyl acetate (7:3) to ethyl acetate to give the expected product as a white solid (0.482 g, 2.28 mmol, 36% yield). ^{1}H NMR (500 MHz, DMSO-d_6) δ ppm 7.39 - 7.52 (m, 4 H), 7.53 - 7.66 (m, 1 H), 7.92 - 8.04 (m, 1 H); ^{13}C NMR (126 MHz, DMSO-d_6) δ ppm 127.65, 129.57, 130.27, 130.41, 130.43, 130.90, 151.58, 170.10; mp 191-192 °C; MS (ESI): *m/z* 211.99 $(M+H)^+$, 252.89 $(M+H+CH_3CN)^+$; 98%.

5-(3-Bromophenyl)-1,3,4-oxadiazol-2-amine (36) was prepared according to General Procedure 3 starting from 2-(3-bromobenzoyl)hydrazinecarbothioamide (**24**, 0.506 g, 1.85 mmol). The crude product was triturated with DCM/MeOH and filtered to afford a yellow solid as the pure product (0.225 g, 0.890 mmol, 48% yield) ^{1}H NMR (500 MHz, DMSO-d_6) δ ppm 7.34 (br. s, 2 H), 7.49 (t, *J*=7.9 Hz, 1 H), 7.71 (ddd, *J*=8.0, 2.8, 0.9 Hz, 1 H), 7.78 (ddd, *J*=7.9, 2.5, 0.9 Hz, 1 H), 7.90 (t, *J*=1.6 Hz, 1 H); ^{13}C NMR (126 MHz, DMSO-d_6) δ ppm 122.21, 123.94, 126.45, 127.29, 131.50, 132.97, 155.98, 164.08; mp 240-243°C; MS (ESI): *m/z* 239.84 $(M+H)^+$, 280.87 $(M+H+CH_3CN)^+$; 98%.

5-(3-(Trifluoromethyl)phenyl)-1,3,4-oxadiazol-2-amine (37) was prepared according to General Procedure 3 starting from 2-(3-(trifluoromethyl)benzoyl)hydrazinecarbothioamide (**25**, 2.00 g, 7.60 mmol). The precipitate was triturated with ethyl acetate and filtered. The resulting solid was purified by flash chromatography on silica gel using DCM:MeOH (98:2 to 97:3) to afford the product as a white solid (0.741 g, 3.23 mmol, 43% yield). ^{1}H NMR (500 MHz, DMSO-d_6) δ ppm 7.39 (s, 2 H), 7.78 (t, *J*=7.9 Hz, 1 H), 7.87 (d, *J*=7.9 Hz, 1 H), 8.01 (s, 1 H), 8.08 (d, *J*=7.9 Hz, 1 H); ^{13}C NMR (126 MHz, DMSO-d_6) δ ppm 121.16, 123.70 (d, $^{1}J(C,F)$=270.4 Hz, 1 C), 125.35, 126.73 (q, $^{3}J(C,F)$=3.7 Hz, 1 C), 128.80, 129.79 (q, $^{2}J(C,F)$=31.2 Hz, 1 C), 130.67, 156.17, 164.19; mp 219-224 °C; MS (ESI): *m/z* 229.95 $(M+H)^+$, 270.88 $(M+H+CH_3CN)^+$; 99%.

3-(5-Amino-1,3,4-oxadiazol-2-yl)benzonitrile (38) was prepared according to General Procedure 3 starting from 2-(3-cyanobenzoyl)hydrazinecarbothioamide (**26**, 0.500 g, 2.27 mmol). The crude product was purified by flash-chromatography on silica gel using ethyl acetate:THF (9:1). The resulting yellow solid was triturated with ethyl acetate and a few drops of MeOH. The suspension was filtered to give the product as yellow solid (80 mg, 0.430 mmol,

19% yield). ^{1}H NMR (500 MHz, DMSO-d_6) δ ppm 7.40 (s, 2 H), 7.74 (t, *J*=7.9 Hz, 1 H), 7.96 (d, *J*=7.9 Hz, 1 H), 8.08 (d, *J*=7.9 Hz, 1 H), 8.13 (s, 1 H); ^{13}C NMR (126 MHz, DMSO-d_6) δ ppm 112.43, 117.97, 125.52, 128.26, 129.36, 130.59, 133.65, 155.82, 164.23; mp 242-244; MS (ESI): *m/z* 227.94 $(M+H+CH_3CN)^+$; 99%.

5-(3-(Trifluoromethoxy)phenyl)-1,3,4-oxadiazol-2-amine (39) was prepared according to General Procedure 3 starting from 2-(3-(trifluoromethoxy)benzoyl)hydrazinecarbothioamide (**27**, 0.500 g, 1.79 mmol). The product was obtained as yellow solid (90 mg, 0.349 mmol, 20% yield). ^{1}H NMR (500 MHz, DMSO-d_6) δ ppm 7.37 (s, 2 H), 7.52 (d, *J*=8.2 Hz, 1 H), 7.63 - 7.71 (m, 2 H), 7.81 (dt, *J*=7.8, 1.3 Hz, 1 H); ^{13}C NMR (126 MHz, DMSO-d_6) δ ppm 116.98, 121.01 (t, $^{1}J(C,F)$=257.50 Hz, 1 C), 122.72, 123.99, 126.38, 131.65, 148.68 (q, $^{3}J(C,F)$=1.80 Hz, 1 C), 156.30, 164.30; mp 197-200°C; MS (ESI): *m/z* 286.87 $(M+H+CH_3CN)^+$; 95%.

5-(3-Methoxyphenyl)-1,3,4-oxadiazol-2-amine (40) was prepared according to General Procedure 3 starting from 2-(3-methoxybenzoyl)hydrazinecarbothioamide (**28**, 0.500 g, 2.22 mmol). The crude product was purified by flash-chromatography using ethyl acetate to obtain the pure product as a white solid (152 mg, 0.795 mmol, 36% yield). ^{1}H NMR (500 MHz, DMSO-d_6) δ ppm 3.81 (s, 3 H), 7.07 (dd, *J*=8.20, 2.52 Hz, 1 H), 7.25 (s, 2 H), 7.29 (dd, *J*=2.52, 1.26 Hz, 1 H), 7.37 (dt, *J*=7.80, 1.14 Hz, 1H), 7.44 (t, *J*=7.88 Hz, 1 H); ^{13}C NMR (126 MHz, DMSO-d_6) δ ppm 55.23, 109.83, 116.34, 117.33, 125.57, 130.48, 157.18, 159.53, 163.86; mp 192-195°C; MS (ESI): *m/z* 192.02 $(M+H)^+$; 99%.

5-(4-Tolyl)-1,3,4-oxadiazol-2-amine (41) was prepared according to General Procedure 3 starting from 2-(3-(methyl)benzoyl)hydrazinecarbothioamide (**29**, 0.500 g, 2.39 mmol). The crude product was recrystallized from ethanol to obtaine the product as a pale yellow solid (86

mg, 0.466 mmol, 20% yield). ^{1}H NMR (500 MHz, DMSO-d_6) δ ppm 2.37 (s, 3 H), 7.21 (s, 2 H), 7.27 - 7.34 (m, 1 H), 7.41 (t, *J*=7.6 Hz, 1 H), 7.56 - 7.60 (m, 1 H), 7.60 - 7.62 (m, 1 H); ^{13}C NMR (126 MHz, DMSO-d_6) δ ppm 20.87, 122.19, 124.31, 125.39, 129.11, 130.99, 138.54, 157.37, 163.78; mp 213-216 °C; MS (ESI): *m/z* 176.06 $(M+H)^+$, 217.07 $(M+H+CH_3CN)^+$; 96%.

5-(3-(*Tert*-butyl)phenyl)-1,3,4-oxadiazol-2-amine (42) was prepared according to General Procedure 3 starting from 3-(tert-butyl)benzoyl) thiosemiamidecarbazide (**30**, 1.00 g, 3.98 mmol). The quenched reaction mixture was extracted twice with ethyl acetate. The combined organic phases were washed with a saturated solution of $NaHCO_3$ and brine. The organic layer was dried over $MgSO_4$ and filtered. Heptane was added and ethyl acetate was evaporated to give a yellow suspension. The suspension was filtered and the cake washed with heptane/ethyl acetate to yield a white solid as the pure product (0.265 g, 1.22 mmol, 31% yield). ^{1}H NMR (500 MHz, DMSO-d_6) δ ppm 1.31 (s, 9 H), 7.23 (s, 2 H), 7.45 (t, *J*=7.7 Hz, 1 H), 7.55 (d, *J*=7.9 Hz, 1 H), 7.61 (d, *J*=7.6 Hz, 1 H), 7.79 (s, 1 H); ^{13}C NMR (126 MHz, DMSO-d_6) δ ppm 30.90 (3 C), 34.48, 121.49, 122.36, 124.15, 127.48, 129.04, 151.60, 157.59, 163.80; mp 216-219°C; MS (ESI): *m/z* 218.12 $(M+H)^+$, 259.09 $(M+H+CH_3CN)^+$; 96%.

2-(3-(Trifluoromethyl)phenyl)-1,3,4-oxadiazole (47)[37] A sealed reaction vial was charged with 3-(trifluoromethyl)benzohydrazide (**43**, 0.400 g, 1.96 mmol) and triethyl orthoformate (4.00 mL, 24.0 mmol). The mixture was heated under an argon atmosphere for 2 h at 160 °C. The reaction mixture was poured into a precooled saturated aqueous solution of Na_2CO_3 while stirring vigorously at 0 °C. The aqueous phase was extracted twice with ethyl acetate and the combined organic phases were washed with brine (2 times). The organic phase was dried over $MgSO_4$ and concentrated. The resulting yellow oil was adsorbed on silica gel and purified by flash chromatography using hexane/ethyl acetate (95:5) to (8:2) to give a colorless oil, which

crystallized in the fridge (0.262 g, 1.22 mmol, 62% yield). ^{1}H NMR (500 MHz, DMSO-d_6) δ ppm 7.87 (t, *J*=7.9 Hz, 1 H), 8.00 - 8.04 (m, 1 H), 8.26 (s, 1 H), 8.30 - 8.34 (m, 1 H), 9.44 (s, 1 H); ^{13}C NMR (126 MHz, DMSO-d_6) δ ppm 123.6 (q, $^{1}J(C,F)$=272.2 Hz, 1 C), 123.0 (q, $^{3}J(C,F)$=3.7 Hz, 1 C), 124.3, 128.5 (q, $^{3}J(C,F)$=3.7 Hz, 1 C), 130.1 (q, $^{2}J(C,F)$=32.1 Hz, 1 C), 130.7, 130.9, 155.0, 162.6; mp 35°C; MS (ESI): *m/z* 255,91 $(M+ H+CH_3CN)^+$; 97%.

2-Methyl-5-(3-(trifluoromethyl)phenyl)-1,3,4-oxadiazole (48)[37] 3-(Trifluoromethyl)-benzohydrazide (**43**, 0.500 g, 2.45 mmol) was filled into a sealed reaction vial. Triethyl orthoacetate (8.00 mL, 43.4 mmol) was added to give a clear solution. The solution was heated to 150 °C in a metal block over-night. The reaction mixture was poured into a precooled saturated solution of Na_2CO_3 while stirring vigorously at 0 °C. The water phase was extracted twice with ethyl acetate and the combined organic layers were washed with brine. The organic phase was dried over $MgSO_4$ and concentrated to obtain a pale yellow oil. Scratching with a spatula afforded a white solid. The white solid was triturated with hexane and filtered. The resulting cake was washed with hexane to give the pure product as white crystals (0.230 g, 1.01 mmol, 41% yield). ^{1}H NMR (500 MHz, DMSO-d_6) δ ppm 2.61 (s, 3 H), 7.84 (t, *J*=7.9 Hz, 1 H), 7.99 (d, *J*=7.9 Hz, 1 H), 8.19 (s, 1 H), 8.26 (d, *J*=7.9 Hz, 1 H); ^{13}C NMR (126 MHz, DMSO-d_6) δ ppm 10.33, 123.58 (q, $^{1}J(C,F)$=273.1 Hz, 1 C), 128.19 (q, $^{3}J(C,F)$=3.7 Hz, 1 C), 130.06 (q, $^{2}J(C,F)$=33.9, Hz, 1 C), 130.23, 130.83, 162.81, 164.49; mp 79-82°C; MS (ESI): *m/z* 228.96 $(M+H)^+$, 270.00 $(M+H+CH_3CN)^+$.

2-Methoxy-5-(3-(trifluoromethyl)phenyl)-1,3,4-oxadiazole (49)[36] Methyl 2-(3-(trifluoromethyl)benzoyl)hydrazinecarboxylate (**44**, 0.500 g, 1.91 mmol) and Burgess reagent (0.680 g, 2.86 mmol) were dissolved in dry THF (9 mL) in a MW vial flushed with argon. The reaction mixture was heated in the MW for 2 min (dynamic heating 100W max power, 150 °C

safe temperature). The reaction mixture was poured into a saturated aqueous solution of $NaHCO_3$. The aqueous phase was extracted twice with ethyl acetate. The combined organic layers were percolated through a filter loaded with silica gel. The filtrate was concentrated to give a yellow oil. The oil was triturated with diethyl ether to afford a suspension. The solid was removed by filtration. The filtrate was adsorbed on silica gel and purified by flash chromatography with DCM:hexane (1:1) to yield the product as colorless needles (167 mg, 0.684 mmol, 36% yield). ^{1}H NMR (500 MHz, DMSO-d_6) δ ppm 4.20 (s, 3 H), 7.82 (t, *J*=7.9 Hz, 1 H), 7.96 (d, *J*=7.9 Hz, 1 H), 8.11 (s, 1 H), 8.17 (d, *J*=7.9 Hz, 1 H); ^{13}C NMR (126 MHz, DMSO-d_6) δ ppm 59.88, 121.94 (q, $^3J(C,F)$=3.7 Hz, 1 C), 123.58 (d, $^1J(C,F)$=272.2 Hz, 1 C), 124.64, 127.89 (q, $^3J(C,F)$=3.7 Hz, 1 C), 129.61, 130.01 (d, $^2J(C,F)$=32.1 Hz, 1 C), 130.75, 158.64, 166.11; mp 42-43 °C; HRMS: *m/z* calcd 245.0532 $(M+H)^+$ found 245.0557.

2-(Trifluoromethyl)-5-(3-(trifluoromethyl)phenyl)-1,3,4-oxadiazole (50)[36] *N*'-(2,2,2-trifluoroacetyl)-3-(trifluoromethyl)benzohydrazide (**45**, 0.500 g, 1.66 mmol) and Burgess reagent (0.595 g, 2.50 mmol) were dissolved in dry THF (9 mL) in a MW vial flushed with argon. The reaction mixture was heated in the MW for 2 min (dynamic heating 100W max power, 150 °C safe temperature). The reaction mixture was poured into a saturated aqueous solution of $NaHCO_3$. The aqueous phase was extracted twice with ethyl acetate. The combined organic layers were percolated through a filter loaded with silica gel. The filtrate was concentrated to give a yellow oil. The oil was triturated with ethyl acetate and DCM. The resulting suspension was cooled in the fridge and filtered. The filtrate was adsorbed on silica gel and purified by flash chromatography using a gradient of hexane/ethyl acetate (95:5) to (70:30) to yield a yellow oil. The oil crystallized in the fridge to give the pure product as yellow needles (205 mg, 0.730 mmol, 43% yield). ^{1}H NMR (500 MHz, DMSO-d_6) δ ppm 7.91 (t, *J*=7.9 Hz, 1 H), 8.10 (d, *J*=7.9

Hz, 1 H), 8.31 (s, 1 H), 8.39 (d, *J*=7.9 Hz, 1 H); ^{13}C NMR (126 MHz, DMSO-d_6) δ ppm 116.14 (d, $^{1}J(C,F)$=272.2 Hz, 1 C), 123.45 (d, $^{1}J(C,F)$=271.3 Hz, 1 C), 123.26, 123.71 (q, $^{3}J(C,F)$=3.7 Hz, 1 C), 129.56 (q, $^{3}J(C,F)$=3.7 Hz, 1 C), 130.20 (q, $^{2}J(C,F)$=32.1 Hz, 1 C), 131.05, 131.40, 154.33 (d, $^{2}J(C,F)$=44.0 Hz, 1 C), 164.92; mp 25 °C; MS (ESI): *m/z* not found $(M+H)^+$, 99%; HRMS: *m/z* calcd 283.0300 $(M+H)^+$ found 283.0313.

***N*-methyl-5-(3-(trifluoromethyl)phenyl)-1,3,4-oxadiazol-2-amine (51)**[40] *N*-methylhydrazine-carbothioamide (186 mg, 1.770 mmol) was dissolved in DCM (8 ml). 3-(trifluoromethyl)benzoyl chloride (**17**, 0.250 mL, 1.770 mmol) was added. The resulting suspension was stirred for 15 min at RT, then EDC (0,500 mL, 3,81 mmol) was added to give a yellow solution. The solution was stirred for 24 h at RT. Another amount of EDC (0.25 ml, 1.905 mmol) was added and the solution stirred over night at 40 °C. The reaction mixture was added dropwise to an aqueous citric acid solution (10%). The aqueous layer was extracted with ethyl acetate (3 times). The combined ethyl acetate layers were washed with saturated aqueous $NaHCO_3$ solution (2 times) and brine (2 times). The organic layer was concentrated to dryness and purified by flash-chromatography (hexane/ethyl acetate 1:1) to give the product as white solid (60 mg, 0,247 mmol, 14% yield). ^{1}H NMR (500 MHz, DMSO-*d6*) δ ppm 2.88 (d, J=4.7 Hz, 3 H) 7.73 - 7.81 (m, 2 H) 7.88 (dt, J=7.9, 0.8 Hz, 1 H) 8.03 (s, 1 H) 8.08 - 8.12 (m, 1 H); ^{13}C NMR (126 MHz, DMSO-*d6*) δ ppm 28.99, 121.22 (q, $^{3}J(C,F)$=3.7 Hz, 1 C), 124.78 (d, $^{1}J(C,F)$=272.2 Hz, 1 C), 122.62, 125.28, 126.79 (q, $^{3}J(C,F)$=3.7 Hz, 1 C), 128.88, 129.92 (q, $^{2}J(C,F)$=33.9 Hz, 1 C), 130.65, 156.46, 164.42; mp 190-192°C; MS (ESI): *m/z* 243,89 $(M+H)^+$, 96%

5-(3-(Trifluoromethyl)phenyl)-1,3,4-oxadiazole-2-carboxamide (52)[39] Ethyl 5-(3-(trifluoromethyl)phenyl)-1,3,4-oxadiazole-2-carboxylate (**46**, 0.800 g, 2.80 mmol) was dissolved in MeOH (6 mL) and diethyl ether (3 mL) in a sealed reaction vial. Ammonia in MeOH (4.00

mL, 28.0 mmol) was added, the reaction mixture was agitated and aged at RT without stirring for 48 h. The reaction mixture was concentrated to dryness to give the product as white solid (720 mg, 2,80 mmol, 100 % yield). ^{1}H NMR (500 MHz, DMSO-d_6) δ ppm 7.90 (t, *J*=7.9 Hz, 1 H), 8.07 (d, *J*=7.9 Hz, 1 H), 8.30 (br. s, 1 H), 8.34 (s, 1 H), 8.39 (d, *J*=7.9 Hz, 1 H), 8.74 (br. s, 1 H); ^{13}C NMR (126 MHz, DMSO-d_6) δ ppm 123.57 (q, $^{2}J(C,F)$=272.2 Hz, 1 C), 123.45 (q, $^{3}J(C,F)$=4.6 Hz, 1 C), 124.04, 128.98 (q, $^{3}J(C,F)$=4.6 Hz, 1 C), 130.12 (q, $^{2}J(C,F)$=32.9 Hz, 1 C), 130.92, 130.99, 154.27, 158.83, 163.75; mp: 151-153 °C; MS (ESI): *m/z* not found $(M+H)^+$, 98%; HRMS: calcd *m/z* 258.0484 $(M+H)^+$ found 258.0494.

5-(3-(Trifluoromethyl)phenyl)-1,3,4-oxadiazol-2(*3H*)-one (53)[41] 3-(Trifluoromethyl) benzohydrazide (**43**, 0.500 g, 2.45 mmol) was dissolved in DCM (25 mL) and triethylamine (0.512 mL, 3.67 mmol). Carbonyldiimidazole (0.596 g, 3.67 mmol) was added under constant stirring. The reaction mixture was aged at RT for 30 min. The reaction mixture was washed with a 5% aqueous solution of citric acid (2 times) and twice with brine. The organic layer was dried over $MgSO_4$, filtered and concentrated to give a white solid. The solid was triturated with DCM/hexane, filtered and the resulting cake was washed with DCM/hexane to afford the product as a white solid (0.206 g, 0.895 mmol, 37% yield). ^{1}H NMR (500 MHz, DMSO-d_6) δ ppm 7.80 (t, *J*=7.9 Hz, 1 H), 7.94 (d, *J*=7.9 Hz, 1 H), 8.00 (s, 1 H), 8.08 (d, *J*=7.9 Hz, 1 H), 12.75 (br. s, 1 H); ^{13}C NMR (126 MHz, CHLOROFORM-*d*) δ ppm 123.40 (q, $^{1}J(C,F)$=271.3 Hz, 1 C), 122.74 (q, $^{3}J(C,F)$=3.7 Hz, 1 C), 124.61, 128.29 (q, $^{3}J(C,F)$=3.7 Hz, 1 C), 128.84, 129.74, 131.81 (q, $^{2}J(C,F)$=33.0 Hz, 1 C), 154.09, 154.67; mp 112-123 °C; HRMS: *m/z* calcd 231.0375 found 231.0380.

ASSOCIATED CONTENT

Supporting Information Experimental protocols for the expression and purification of PqsR constructs, the biotinylation and immobilization of PqsR, ITC experiments as well as synthesis of intermediates. This material is available free of charge via the Internet at http://pubs.acs.org.

AUTHOR INFORMATION

Corresponding Author

*E-mail: rolf.hartmann@helmholtz-hzi.de

Author Contributions

The manuscript was written through contributions of all authors. All authors have given approval to the final version of the manuscript.

Present Address

†AstraZeneca R&D, Protein Structure and Biophysics, Mereside, Alderley Park, SK10 4TG, UK

‡MIP Pharma GmbH, Kirkler Straße 41, 66440 Blieskastel, Germany

Notes

The authors declare no competing financial interest.

ACKNOWLEDGMENT

The authors would like to thank Simone Amann for performing the in-vitro assays, Dr. Johannes C. de Jong for synthesis of HHQ and HHQ-*d4*, Michael Hoffmann, Dr. Stefan Boettcher and Dr. Josef Zapp for assistance with chemical analytics and Meghan Hattarki and Lesley Pearce for assisting during SPR experiments. The *P. aeruginosa* strain PA14 and its isogenic transposon mutant strains were obtained from Prof. Dr. Susanne Häussler (Twincore Hannover, Germany)

and HQNO from Prof. Dr. Friedrich Hammerschmidt (Institute of Organic Chemistry, Vienna, Austria)

ABBREVIATIONS

QS quorum sensing; PqsR Pseudomonas quorum sensing receptor; LBD ligand binding domain; PQS Pseudomonas Quinolone Signal, HHQ 2-heptyl-4(1*H*)-quinolone, SPR surface plasmon resonance, ITC isothermal titration calorimetry, INPHARMA interligand NOE for pharmacophore mapping

REFERENCES

(1) Williams, P.; Winzer, K.; Chan, W. C.; Cámara, M. Look who's talking: communication and quorum sensing in the bacterial world. *Philos. Trans. R. Soc., B* **2007**, *362,* 1119–1134.

(2) Whitehead, N. A.; Barnard, A. M. L.; Slater, H.; Simpson, N. J. L.; Salmond, G. P. C. Quorum-sensing in Gram-negative bacteria. *FEMS Microbiol. Rev*. **2001**, *25,* 365–404.

(3) Bertrand, X.; Thouverez, M.; Patry, C.; Balvay, P.; Talon, D. *Pseudomonas aeruginosa*: antibiotic susceptibility and genotypic characterization of strains isolated in the intensive care unit. *Clin. Microbiol. Infect.* **2001**, *7,* 706–708.

(4) Vincent, J. L.; Bihari, D. J.; Suter P. M.; Bruining H. A.; White, J.; Nicolas-Chanoin, M.H.; Wolff, M.; Spencer, R.C.; Hemmer, M. The prevalence of nosocomial infection in intensive care units in Europe: Results of the European prevalence of infection in intensive care (epic) study. *J. Am. Med. Assoc.* **1995**, *274,* 639–644.

(5) Koch, C.; Høiby N. Pathogenesis of cystic fibrosis. *The Lancet* **1993**, *341,* 1065–1069.

(6) Walters, M. C.; Roe, F.; Bugnicourt, A.; Franklin, M. J.; Stewart, P. S. Contributions of Antibiotic Penetration, Oxygen Limitation, and Low Metabolic Activity to Tolerance of *Pseudomonas aeruginosa* Biofilms to Ciprofloxacin and Tobramycin. *Antimicro. Agents Chemother*. **2003**, *47,* 317–323.

(7) Aloush, V.; Navon-Venezia, S.; Seigman-Igra, Y.; Cabili, S.; Carmeli, Y. Multidrug-Resistant *Pseudomonas aeruginosa*: Risk Factors and Clinical Impact. *Antimicro. Agents Chemother.* **2006**, *50,* 43–48.

(8) Boucher, H. W.; Talbot, G. H.; Bradley, J. S.; Edwards, J. E.; Gilbert, D.; Rice, L. B.; Scheld, M.; Spellberg, B.; Bartlett, J. Bad Bugs, No Drugs: No ESKAPE! An Update from the Infectious Diseases Society of America. *Clin. Infect. Dis.* **2009**, *48,* 1–12.

(9) Gambello, M. J.; Iglewski, B. H. Cloning and characterization of the *Pseudomonas aeruginosa* lasR gene, a transcriptional activator of elastase expression. *J. Bacteriol.* **1991**, *173,* 3000–3009.

(10) Passador, L.; Cook, J. M.; Gambello, M. J.; Rust, L.; Iglewski, B. H. Expression of *Pseudomonas aeruginosa* virulence genes requires cell-to-cell communication. *Science* **1993**, *260,* 1127–1130.

(11) Ochsner, U. A.; Koch, A. K.; Fiechter, A.; Reiser, J. Isolation and characterization of a regulatory gene affecting rhamnolipid biosurfactant synthesis in *Pseudomonas aeruginosa*. *J. Bacteriol.* **1994**, *176,* 2044–2054.

(12) Ochsner, U. A.; Reiser, J. Autoinducer-mediated regulation of rhamnolipid biosurfactant synthesis in *Pseudomonas aeruginosa*. *Proc. Natl. Acad. Sci. U.S.A.* **1995**, *92,* 6424–6428.

(13) Pesci, E. C.; Milbank, J. B. J.; Pearson, J. P.; McKnight, S.; Kende, A. S.; Greenberg, E. P.; Iglewski, B. H. Quinolone signaling in the cell-to-cell communication system of *Pseudomonas aeruginosa*. *Proc. Natl. Acad. Sci. U.S.A.* **1999**, *96,* 11229–11234.

(14) Cao, H.; Krishnan, G.; Goumnerov, B.; Tsongalis, J.; Tompkins, R.; Rahme, L. G. A quorum sensing-associated virulence gene of *Pseudomonas aeruginosa* encodes a LysR-like transcription regulator with a unique self-regulatory mechanism. *Proc. Natl. Acad. Sci. U.S.A.* **2001**, *98,* 14613–14618.

(15) Diggle, S. P.; Lumjiaktase, P.; Dipilato, F.; Winzer, K.; Kunakorn, M.; Barrett, D. A.; Chhabra, S. R.; Cámara, M.; Williams, P. Functional Genetic Analysis Reveals a 2-Alkyl-4-Quinolone Signaling System in the Human Pathogen *Burkholderia pseudomallei* and Related Bacteria. *Chem. Biol*. **2006**, *13,* 701–710.

(16) Wade, D. S.; Calfee, M. W.; Rocha, E. R.; Ling, E. A.; Engstrom, E.; Coleman, J. P.; Pesci, E. C. Regulation of Pseudomonas Quinolone Signal Synthesis in *Pseudomonas aeruginosa*. *J. Bacteriol.* **2005**, *187,* 4372–4380.

(17) Xiao, G.; Déziel, E.; He, J.; Lépine, F.; Lesic, B.; Castonguay, M.-H.; Milot, S.; Tampakaki, A. P.; Stachel, S. E.; Rahme, L. G. MvfR, a key *Pseudomonas aeruginosa* pathogenicity LTTR-class regulatory protein, has dual ligands. *Mol. Microbiol.* **2006**, *62,* 1689–1699.

(18) Diggle, S. P.; Winzer, K.; Chhabra, S. R.; Worrall, K. E.; Cámara, M.; Williams, P. The *Pseudomonas aeruginosa* quinolone signal molecule overcomes the cell density-dependency of the quorum sensing hierarchy, regulates rhl-dependent genes at the onset of stationary phase and can be produced in the absence of LasR. *Mol. Microbiol.* **2003**, *50,* 29–43.

(19) Gallagher, L. A.; McKnight, S. L.; Kuznetsova, M. S.; Pesci, E. C.; Manoil, C. Functions Required for Extracellular Quinolone Signaling by *Pseudomonas aeruginosa*. *J. Bacteriol.* **2002**, *184,* 6472–6480.

(20) Déziel, E.; Lépine, F.; Milot, S.; He, J.; Mindrinos, M. N.; Tompkins, R. G.; Rahme, L. G. Analysis of *Pseudomonas aeruginosa* 4-hydroxy-2-alkylquinolines (HAQs) reveals a role for 4-hydroxy-2-heptylquinoline in cell-to-cell communication. *Proc. Natl. Acad. Sci. U.S.A.* **2004**, *101,* 1339–1344.

(21) Yang, L.; Nilsson, M.; Gjermansen, M.; Givskov, M.; Tolker-Nielsen, T. Pyoverdine and PQS mediated subpopulation interactions involved in *Pseudomonas aeruginosa* biofilm formation. *Mol. Microbiol.* **2009**, *74,* 1380–1392.

(22) Hartman, G.; Wise, R. Quorum sensing: potential means of treating Gram-negative infections? *The Lancet* **1998**, *351,* 848–849.

(23) Hentzer, M.; Wu, H.; Andersen, J. B.; Riedel, K.; Rasmussen, T. B.; Bagge, N.; Kumar, N.; Schembri, M. A.; Song, Z.; Kristoffersen, P.; Manefield, M.; Costerton, J. W.; Molin, S.; Eberl, L.; Steinberg, P.; Kjelleberg, S.; Hoiby, N.; Givskov, M. Attenuation of *Pseudomonas aeruginosa* virulence by quorum sensing inhibitors. *EMBO J.* **2003**, *22,* 3803–3815.

(24) Imperi, F.; Massai, F.; Facchini, M.; Frangipani, E.; Visaggio, D.; Leoni, L.; Bragonzi, A.; Visca, P. Repurposing the antimycotic drug flucytosine for suppression of Pseudomonas aeruginosa pathogenicity. *Proc. Natl. Acad. Sci. U.S.A*. **2013**, *110,* 7458–7463.

(25) Lu, C.; Kirsch, B.; Zimmer, C.; Jong, J. C. de; Henn, C.; Maurer, C. K.; Müsken, M.; Häussler, S.; Steinbach, A.; Hartmann, R. W. Discovery of Antagonists of PqsR, a Key Player in 2-Alkyl-4-quinolone-Dependent Quorum Sensing in *Pseudomonas aeruginosa*. *Chem. Biol.* **2012**, *19,* 381–390.

(26) Leeson, P. D.; Springthorpe, B. The influence of drug-like concepts on decision-making in medicinal chemistry. *Nat. Rev. Drug Discovery* **2007**, *6,* 881–890.

(27) Waldrop, G. L. Smaller Is Better for Antibiotic Discovery. *ACS Chem. Biol*. **2009**, *4,* 397–399.

(28) Hajduk, P. J.; Greer, J. A decade of fragment-based drug design: strategic advances and lessons learned. *Nat. Rev. Drug Discovery* **2007**, *6,* 211–219.

(29) Klein, T.; Henn, C.; Jong, J. C. de; Zimmer, C.; Kirsch, B.; Maurer, C. K.; Pistorius, D.; Müller, R.; Steinbach, A.; Hartmann, R. W. Identification of Small-Molecule Antagonists of the *Pseudomonas aeruginosa* Transcriptional Regulator PqsR: Biophysically Guided Hit Discovery and Optimization. *ACS Chem. Biol.* **2012**, *7*, 1496–1501.

(30) Kurzak, B.; Kozłowski, H.; Farkas, E. Hydroxamic and aminohydroxamic acids and their complexes with metal ions. *Coord. Chem. Rev.* **1992**, *114,* 169–200.

(31) Muri, E. M. F.; Nieto, M. J.; Sindelar, R. D.; Williamson, J. S. Hydroxamic acids as pharmacological agents. *Curr. Med. Chem.* **2002**, *9,* 1631–1653.

(32) Ching Yung Wang. Mutagenicity of hydroxamic acids for *Salmonella typhimurium*. *Mutat. Res., Fundam. Mol. Mech. Mutagen.* **1977**, *56,* 7–12.

(33) Ferrari, S.; Morandi, F.; Motiejunas, D.; Nerini, E.; Henrich, S.; Luciani, R.; Venturelli, A.; Lazzari, S.; Calò, S.; Gupta, S.; Hannaert, V.; Michels, P. A. M.; Wade, R. C.; Costi, M. P. Virtual Screening Identification of Nonfolate Compounds, Including a CNS Drug, as Antiparasitic Agents Inhibiting Pteridine Reductase. *J. Med. Chem.* **2010**, *54,* 211–221.

(34) Rivera, N. R.; Balsells, J.; Hansen, K. B. Synthesis of 2-amino-5-substituted-1,3,4-oxadiazoles using 1,3-dibromo-5,5-dimethylhydantoin as oxidant. *Tetrahedron Lett.* **2006**, *47,* 4889–4891.

(35) Oruç, E. E.; Rollas, S.; Kandemirli, F.; Shvets, N.; Dimoglo, A. S. 1,3,4-Thiadiazole Derivatives. Synthesis, Structure Elucidation, and Structure-Antituberculosis Activity Relationship Investigation. *J. Med. Chem.* **2004**, *47,* 6760–6767.

(36) Brain, C. T.; Paul, J. M.; Loong, Y.; Oakley, P. J. Novel procedure for the synthesis of 1,3,4-oxadiazoles from 1,2-diacylhydrazines using polymer-supported Burgess reagent under microwave conditions. *Tetrahedron Lett.* **1999**, *40,* 3275–3278.

(37) Ainsworth, C.; Hackler, R. E. Alkyl-1,3,4-oxadiazoles. *J. Org. Chem.* **1966**, *31,* 3442–3444.

(38) Huguet, F.; Melet, A.; Alves de Sousa, R.; Lieutaud, A.; Chevalier, J.; Maigre, L.; Deschamps, P.; Tomas, A.; Leulliot, N.; Pages, J.-M.; Artaud, I. Hydroxamic Acids as Potent Inhibitors of FeII and MnII *E.coli* Methionine Aminopeptidase: Biological Activities and X-ray Structures of Oxazole Hydroxamate–EcMetAP-Mn Complexes. *ChemMedChem* **2012**, *7,* 1020–1030.

(39) Dost, J.; Heschel, M.; Stein, J. Zur Herstellung von 1,3,4-Oxadiazol-2-carbonsäurederivaten. *J. Prakt. Chem.* **1985**, *327,* 109–116.

(40) Piatnitski Chekler, E. L.; Elokdah, H. M.; Butera, J. Efficient one-pot synthesis of substituted 2-amino-1,3,4-oxadiazoles. *Tetrahedron Lett.* **2008**, *49,* 6709–6711.

(41) Flechter, J. M.; Fong Tung M.; Hagmann W. K.; Vachal P. Sufonylated Piperazines as Cannabinoid-1 Receptor Modulators. WO2008/024284, **2008**.

(42) Myszka, D. G.; Rich, R. L. Implementing surface plasmon resonance biosensors in drug discovery. *Pharm. Sci. Technol. Today* **2000**, *3,* 310–317.

(43) Giannetti, A. M.; Koch, B. D.; Browner, M. F. Surface plasmon resonance based assay for the detection and characterization of promiscuous inhibitors. *J. Med. Chem.* **2008**, *51,* 574–580.

(44) Perspicace, S.; Banner, D.; Benz, J.; Müller, F.; Schlatter, D.; Huber, W. Fragment-Based Screening Using Surface Plasmon Resonance Technology. *J. Biomol. Screening* **2009**, *14,* 337–349.

(45) Ladbury, J. E.; Klebe, G.; Freire, E. Adding calorimetric data to decision making in lead discovery: a hot tip. *Nat. Rev. Drug Discovery* **2010**, *9,* 23–27.

(46) Ladbury, J. E.; Chowdhry, B. Z. Sensing the heat: the application of isothermal titration calorimetry to thermodynamic studies of biomolecular interactions. *Chem. Biol.* **1996**, *3,* 791–801.

(47) Hopkins, A. L.; Groom, C. R.; Alex, A. Ligand efficiency: a useful metric for lead selection. *Drug Discovery Today* **2004**, *9,* 430–431.

(48) Cugini, C.; Calfee, M. W.; Farrow, J. M.; Morales, D. K.; Pesci, E. C.; Hogan, D. A. Farnesol, a common sesquiterpene, inhibits PQS production in *Pseudomonas aeruginosa*. *Mol. Microbiol.* **2007**, *65,* 896–906.

(49) Nicas, T. I.; Hancock, P. *Pseudomonas aeruginosa* outer membrane permeability: isolation of a porin protein F-deficient mutant. *J. Bacteriol.* **1983**, *153,* 281–285.

(50) Kefala, K.; Kotsifaki, D.; Providaki, M.; Kapetaniou, E. G.; Rahme, L.; Kokkinidis, M. Purification, crystallization and preliminary X-ray diffraction analysis of the C-terminal fragment of the MvfR protein from *Pseudomonas aeruginosa*. *Acta Crystallogr., Sect. F: Struct. Biol. Cryst. Commun.* **2012**, *68,* 695–697.

(51) Xu, N.; Yu, S.; Moniot, S.; Weyand, M.; Blankenfeldt, W. Crystallization and preliminary crystal structure analysis of the ligand-binding domain of PqsR (MvfR), the *Pseudomonas* quinolone signal (PQS) responsive quorum-sensing transcription factor of *Pseudomonas aeruginosa*. *Acta Crystallogr., Sect. F: Struct. Biol. Cryst. Commun.* **2012**, *68,* 1034–1039.

(52) Freire, E. Do enthalpy and entropy distinguish first in class from best in class? *Drug Discovery Today* **2008**, *13,* 869–874

(53) Rubeš, M.; Bludský, O.; Nachtigall, P. Investigation of the Benzene-Naphthalene and Naphthalene–Naphthalene Potential Energy Surfaces: DFT/CCSD(T) Correction Scheme. *ChemPhysChem* **2008**, *9,* 1702–1708.

(54) Sánchez-Pedregal, V. M.; Reese, M.; Meiler, J.; Blommers, M. J. J.; Griesinger, C.; Carlomagno, T. The INPHARMA Method: Protein-Mediated Interligand NOEs for Pharmacophore Mapping. *Angew. Chem., Int. Ed.* **2005**, *117,* 4244–4247.

(55) Cozzi, F.; Cinquini, M.; Annunziata, R.; Dwyer, T.; Siegel, J. S. Polar/π interactions between stacked aryls in 1,8-diarylnaphthalenes. *J. Am. Chem. Soc.* **1992**, *114,* 5729–5733.

(56) Gung, B. W.; Xue, X.; Zou, Y. Enthalpy (ΔH) and Entropy (ΔS) for π-Stacking Interactions in Near-Sandwich Configurations: Relative Importance of Electrostatic, Dispersive, and Charge-Transfer Effects. *J. Org. Chem.* **2007**, *72,* 2469–2475.

(57) Wheeler, S. E.; Houk, K. N. Substituent Effects in the Benzene Dimer are Due to Direct Interactions of the Substituents with the Unsubstituted Benzene. *J. Am. Chem. Soc.* **2008**, *130,* 10854–10855.

(58) Sinnokrot, M. O.; Valeev, E. F.; Sherrill, C. D. Estimates of the Ab Initio Limit for π-π Interactions: The Benzene Dimer. *J. Am. Chem. Soc.* **2002**, *124,* 10887–10893.

(59) Pierce, A. C.; Sandretto, K. L.; Bemis, G. W. Kinase inhibitors and the case for CH…O hydrogen bonds in protein-ligand binding. *Proteins* **2002**, *49,* 567–576.

(60) Rada, B.; Gardina, P.; Myers, T. G.; Leto, T. L. Reactive oxygen species mediate inflammatory cytokine release and EGFR-dependent mucin secretion in airway epithelial cells exposed to *Pseudomonas* pyocyanin. *Mucosal Immunol.* **2011**, *4,* 158–171.

(61) Déziel, E.; Gopalan, S.; Tampakaki, A. P.; Lépine, F.; Padfield, K. E.; Saucier, M.; Xiao, G.; Rahme, L. G. The contribution of MvfR to *Pseudomonas aeruginosa* pathogenesis and quorum sensing circuitry regulation: multiple quorum sensing-regulated genes are modulated without affecting *lasRI*, *rhlRI* or the production of *N*-acyl-L-homoserine lactones. *Mol. Microbiol.* **2005**, *55,* 998–1014.

(62) Hazan, R.; He, J.; Xiao, G.; Dekimpe, V.; Apidianakis, Y.; Lesic, B.; Astrakas, C.; Déziel, E.; Lépine, F.; Rahme, L. G. Homeostatic Interplay between Bacterial Cell-Cell Signaling and Iron in Virulence. *PLoS Pathog.* **2010**, *6,* e1000810 EP.

(63) Merlot, C. Computational toxicology—a tool for early safety evaluation. *Drug Discovery Today* **2010**, *15,* 16–22.

(64) Papalia, G. A.; Leavitt, S.; Bynum, M. A.; Katsamba, P. S.; Wilton, R.; Qiu, H.; Steukers, M.; Wang, S.; Bindu, L.; Phogat, S.; Giannetti, A. M.; Ryan, T. E.; Pudlak, V. A.; Matusiewicz, K.; Michelson, K. M.; Nowakowski, A.; Pham-Baginski, A.; Brooks, J.; Tieman, B. C.; Bruce, B. D.; Vaughn, M.; Baksh, M.; Cho, Y. H.; Wit, M. de; Smets, A.; Vandersmissen, J.; Michiels, L.; Myszka, D. G. Comparative analysis of 10 small molecules binding to carbonic anhydrase II by different investigators using Biacore technology. *Anal. Biochem.* **2006**, *359,* 94–105.

(65) Griffith, K. L.; Wolf, R. E. Measuring beta-galactosidase activity in bacteria: cell growth, permeabilization, and enzyme assays in 96-well arrays. *Biochem. Biophys. Res. Commun.* **2002**, *290,* 397–402.

(66) Storz, M. P.; Maurer, C. K.; Zimmer, C.; Wagner, N.; Brengel, C.; Jong, J. C. de; Lucas, S.; Müsken, M.; Häussler, S.; Steinbach, A.; Hartmann, R. W. Validation of PqsD as an Anti-biofilm Target in *Pseudomonas aeruginosa* by Development of Small-Molecule Inhibitors. *J. Am. Chem. Soc.* **2012**, *134,* 16143–16146.

(67) Essar, D. W.; Eberly, L.; Hadero, A.; Crawford, I. P. Identification and characterization of genes for a second anthranilate synthase in *Pseudomonas aeruginosa*: interchangeability of the two anthranilate synthases and evolutionary implications. *J. Bacteriol.* **1990**, *172,* 884–900.

(68) Lépine, F.; Déziel, E.; Milot, S.; Rahme, L. G. A stable isotope dilution assay for the quantification of the Pseudomonas quinolone signal in *Pseudomonas aeruginosa* cultures. *Biochim. Biophys. Acta, Gen. Subj.* **2003**, *1622,* 36–41.

(69) Lépine, F.; Milot, S.; Déziel, E.; He, J.; Rahme, L. G. Electrospray/mass spectrometric identification and analysis of 4-hydroxy-2-alkylquinolines (HAQs) produced by *Pseudomonas aeruginosa*. *J. Am. Soc. Mass Spectrom*. **2004**, *15,* 862–869.

TABLE OF CONTENTS GRAPHIC